

SIGNAL TRANSDUCTION

GLK-IKK β signaling induces dimerization and translocation of the AhR-ROR γ t complex in IL-17A induction and autoimmune disease

Huai-Chia Chuang¹, Ching-Yi Tsai¹, Chia-Hsin Hsueh¹, Tse-Hua Tan^{1,2*}

Retinoic-acid-receptor-related orphan nuclear receptor γ t (ROR γ t) controls the transcription of interleukin-17A (IL-17A), which plays critical roles in the pathogenesis of autoimmune diseases. Severity of several human autoimmune diseases is correlated with frequencies of germinal center kinase-like kinase (GLK) (also known as MAP4K3)-overexpressing T cells; however, the mechanism of GLK overexpression-induced autoimmunity remains unclear. We report the signal transduction converging on aryl hydrocarbon receptor (AhR)-ROR γ t interaction to activate transcription of the IL-17A gene in T cells. T cell-specific GLK transgenic mice spontaneously developed autoimmune diseases with selective induction of IL-17A in T cells. In GLK transgenic T cells, protein kinase C θ (PKC θ) phosphorylated AhR at Ser³⁶ and induced AhR nuclear translocation. AhR also interacted with ROR γ t and transported ROR γ t into the nucleus. IKK β (inhibitor of nuclear factor κ B kinase β)-mediated ROR γ t Ser⁴⁸⁹ phosphorylation induced the AhR-ROR γ t interaction. T cell receptor (TCR) signaling also induced the novel ROR γ t phosphorylation and subsequent AhR-ROR γ t interaction. Collectively, TCR signaling or GLK overexpression induces IL-17A transcription through the IKK β -mediated ROR γ t phosphorylation and the AhR-ROR γ t interaction in T cells. Our findings suggest that inhibitors of GLK or the AhR-ROR γ t complex could be used as IL-17A-blocking agents for IL-17A-mediated autoimmune diseases.

INTRODUCTION

Autoimmune diseases, which are chronic, debilitating, and life-threatening, arise from immune system overactivation. T helper 17 cells [T_H17, interleukin-17A (IL-17A)-producing CD4⁺ T cells] and IL-17A play critical roles in the pathogenesis of autoimmune diseases (1, 2). Induction of IL-17A occurs in the synovial fluids from rheumatoid arthritis (RA) patients (3) and in the renal biopsies from systemic lupus erythematosus (SLE) patients (1). IL-17A facilitates differentiation of osteoclasts, which lead to arthritis (3). IL-17A also promotes B cell proliferation and class switch recombination, contributing to autoantibody production and autoimmune responses (4). Furthermore, IL-17A overexpression causes tissue damage by inducing infiltration of neutrophils and macrophages through multiple chemokines (1, 2, 5). IL-17A knockout (KO) or IL-17A blockade abolishes disease development in animal autoimmune models such as experimental autoimmune encephalomyelitis (EAE) and collagen-induced arthritis (CIA) (2). Thus, understanding the mechanism(s) controlling IL-17A transcription may lead to the discovery of novel therapeutic targets for autoimmune diseases.

IL-1 β , IL-6, IL-21, and IL-23 facilitate T_H17 differentiation (1, 2, 6, 7). The T_H17 lineage-specific transcription factor ROR γ t binds to the IL-17A promoter and controls IL-17A gene transcription (8, 9). Transforming growth factor- β (TGF- β)-induced Foxp3, a regulatory T cell (T_{reg}) lineage-specific transcription factor, suppresses IL-17A expression by interacting with and inactivating ROR γ t (10, 11). Besides ROR γ t, several non-lineage-specific transcription factors play important roles in regulating IL-17A transcription. IL-6- or IL-23-stimulated signal transducer and activator

of transcription 3 (STAT3) binds to the IL-17A promoter and enhances IL-17A transcription (12, 13). ROCK (Rho-associated, coiled-coil-containing protein kinase)-phosphorylated interferon (IFN) regulatory factor 4 (IRF4) also promotes IL-17A transcription upon TGF- β signaling (14). Basic leucine zipper ATF-like transcription factor (BATF) controls T_H17 differentiation through binding to the intergenic elements between the IL-17A and IL-17F genes, as well as to the IL-21 or IL-22 promoters (15). Krüppel-like factor 4 (KLF4) binds to the IL-17A promoter and contributes to T_H17 differentiation independent of ROR γ t expression (16). Aryl hydrocarbon receptor (AhR) promotes T_H17 polarization by inducing IL-17A transcription (17, 18) and inhibiting the negative regulator STAT1 during T_H17 differentiation (19). Conversely, T cell-specific AhR KO mice have impaired T_H17 differentiation and are resistant to T_H17-mediated experimental autoimmune arthritis (20). Various pathogenic T_H17 subpopulations can be derived in vitro under different conditions (21). Nevertheless, the in vivo roles of these distinct T_H17 subpopulations in the pathogenesis of autoimmune diseases remain unclear.

MAP4K3 (also named GLK) is a mammalian Ste20-like serine/threonine kinase that was first identified as an upstream activator for the c-Jun N-terminal kinase pathway (22, 23). GLK plays an important role in T cell receptor (TCR) signaling by directly phosphorylating and activating PKC θ , leading to activation of IKK β [inhibitor of nuclear factor κ B (NF- κ B) kinase β] and NF- κ B in T cells (24). Moreover, clinical samples from patients with autoimmune diseases, such as SLE, RA, or adult-onset Still's disease, show markedly increased GLK expression in T cells; the frequencies of GLK-expressing T cells are positively correlated with disease severity (24–26). Consistent with the correlation of high levels of GLK expression with autoimmune disease, GLK-deficient mice are resistant to T_H17-mediated EAE induction or CIA induction and display lower T_H17 responses (24, 26). Besides T_H17, differentiation of T_H1 and T_H2 is also impaired in GLK-deficient T cells because of

Copyright © 2018
The Authors, some
rights reserved;
exclusive licensee
American Association
for the Advancement
of Science. No claim to
original U.S. Government
Works. Distributed
under a Creative
Commons Attribution
License 4.0 (CC BY).

¹Immunology Research Center, National Health Research Institutes, Zhunan 35053, Taiwan. ²Department of Pathology and Immunology, Baylor College of Medicine, Houston, TX 77030, USA.

*Corresponding author. Email: ttan@nhri.org.tw

impaired TCR signaling (24). However, it remains unclear how GLK overexpression contributes to multiple human autoimmune diseases. To understand the pathogenic mechanism of GLK overexpression-induced autoimmune diseases, we generated and characterized T cell-specific GLK transgenic (Lck-GLK Tg) mice. Here, we report that GLK signaling induces a novel interaction between AhR and phospho-ROR γ t through PKC θ and IKK β , leading to IL-17A transcriptional activation and autoimmune responses.

RESULTS

Lck-GLK Tg mice develop autoimmune diseases through IL-17A

To study the consequence of GLK overexpression *in vivo*, we generated Lck-GLK Tg mice (fig. S1, A and B). Lck-GLK Tg mice displayed normal development of T cells and B cells (fig. S1, C to H); however, the mice displayed paralysis of the hindlimb and tail, clouding of the eye, or symptoms of proctitis and dermatitis between 8 and 16 weeks of age (fig. S2A). Lck-GLK Tg mice also showed hepatosplenomegaly and enlargement of lymph nodes and kidneys (fig. S2B). Histology staining showed the induction of pneumonia, nephritis, and spleen abnormality in these mice (Fig. 1A). Induction of serum autoantibodies in Lck-GLK Tg mice (Fig. 1B) also suggests the development of autoimmune responses in these mice. To study which proinflammatory cytokines contribute to autoimmune diseases in Lck-GLK Tg mice, we determined serum cytokines via enzyme-linked immunosorbent assay (ELISA). Surprisingly, only IL-17A was selectively induced in the sera of 4-week-old Lck-GLK Tg mice (Fig. 1C), whereas the proinflammatory cytokines IFN- γ and tumor necrosis factor- α (TNF- α) were not induced. Consistently, *in vitro* T_H17 differentiation of Lck-GLK Tg T cells was increased compared to that of wild-type T cells (fig. S2C), whereas *in vitro* T_H1 differentiation of Lck-GLK Tg T cells was unaffected (fig. S2C). Moreover, IL-17A production was induced in unstimulated T cells of Lck-GLK Tg mice compared to that of wild-type mice (fig. S2D). To rule out the potential position effect of the transgene, we also characterized the second Lck-GLK Tg mouse line (Lck-GLK #2) (fig. S1B). The second line of Lck-GLK Tg mice also displayed GLK overexpression in T cells (fig. S1B) and induction of serum IL-17A levels (fig. S2E). These data suggest that GLK overexpression in T cells induces IL-17A production in mice.

To demonstrate the pathogenic role of IL-17A in Lck-GLK Tg mice, we bred Lck-GLK Tg mice with IL-17A-deficient mice. GLK-induced serum IL-17A levels were significantly decreased by IL-17A deficiency, while other inflammatory cytokine levels were unaffected (fig. S3A). Moreover, autoantibody levels were also significantly reduced in Lck-GLK Tg/IL-17A-deficient mice compared to those in Lck-GLK Tg mice (Fig. 1D). Lck-GLK Tg/IL-17A-deficient mice displayed a reduction of infiltrating inflammatory cells in the kidneys, the liver, and the lung, while showing normal distribution of white pulp and red pulp in the spleen, compared to those in Lck-GLK Tg mice (fig. S3B). The data suggest that IL-17A contributes to autoimmune responses in Lck-GLK Tg mice. To further demonstrate that the induction of IL-17A is due to GLK overexpression, we treated Lck-GLK T cells with GLK short hairpin RNA (shRNA). IL-17A overproduction was abolished by GLK shRNA knockdown in T cells purified from Lck-GLK Tg mice (Fig. 1E). These results demonstrate that GLK overexpression induces

IL-17A overproduction and subsequent autoimmune phenotypes in mice.

GLK induces IL-17A transcription by activating AhR and ROR γ t

Next, we studied the mechanism of GLK-induced IL-17A in T cells. The levels of IL-23 receptor and phosphorylated STAT3 were not increased in T cells of Lck-GLK Tg mice (fig. S4, A and B), suggesting that IL-17A overexpression is not due to enhancement of IL-23 signaling or IL-6/STAT3 signaling. Consistent with the IL-17A protein levels, mRNA levels of IL-17A were significantly increased in the purified T cells of Lck-GLK Tg mice compared to those of wild-type mice (Fig. 2A). We studied whether IL-17A overexpression is due to transcriptional activation of the IL-17A promoter. IL-17A promoter activities in Jurkat T cells were enhanced by GLK overexpression but not by GLK kinase-dead (K45E) mutant (Fig. 2B). Next, we studied the bindings of individual IL-17A transcription factors to the IL-17A promoter (Fig. 2, C and D). ChIP analyses showed that bindings of AhR and ROR γ t (–877) to the IL-17A promoter were induced in T cells of Lck-GLK Tg mice (Fig. 2D), whereas bindings of STAT3, IRF4, KLF4, and BATF to the IL-17A promoter were not enhanced (Fig. 2D). The binding of ROR γ t to the –120 region of the IL-17A promoter was not significantly induced (Fig. 2D); others reported similar findings (27, 28). Consistent with ChIP data, mutation of the AhR-binding element or the ROR γ t-binding site (–877) abolished the GLK-enhanced IL-17A reporter activity, whereas mutation of the STAT3-binding site (Fig. 2E) or the ROR γ t-binding site (–120) did not affect the GLK-induced IL-17A reporter activity (fig. S4C). Notably, GLK overexpression induced AhR response element-driven reporter (XRE-Luc) activity (Fig. 2F), whereas ROR γ t (–877) or STAT3 response element-driven reporter (ROR γ t-Luc or SIE-Luc) activity was unaffected (Fig. 2F). These results suggest that GLK signaling induces IL-17A transcription by activating AhR and maybe ROR γ t.

GLK controls IL-17A production and autoimmune responses through AhR

To further demonstrate the role of AhR in promoting IL-17A production in Lck-GLK Tg mice, we bred Lck-GLK Tg mice with T cell-specific AhR conditional KO (AhR cKO: AhR^{fl/fl};CD4-Cre) mice. Serum IL-17A levels were drastically reduced in Lck-GLK/AhR cKO (Lck-GLK;AhR^{fl/fl};CD4-Cre) mice, whereas serum TNF- α and IFN- γ levels were unaffected by AhR deficiency (Fig. 3A). Levels of ANA, anti-dsDNA antibody, and RF were also decreased in Lck-GLK/AhR cKO mice compared to those in Lck-GLK Tg mice (fig. S5A). Histology staining showed that AhR KO abolished induction of nephritis and spleen abnormality in Lck-GLK Tg mice (fig. S5B). AhR KO also suppressed infiltration of inflammatory immune cells in the liver of Lck-GLK Tg mice (fig. S5B). The data indicate that AhR plays a critical role in the IL-17A overproduction and autoimmune responses in Lck-GLK Tg mice.

PKC θ phosphorylates AhR at Ser³⁶ and induces AhR nuclear translocation

Next, we studied the mechanism of GLK-induced AhR binding to the IL-17A promoter. The confocal images (using two different anti-AhR antibodies; Fig. 3B and fig. S5C) and subcellular fractionation experiments (Fig. 3C) showed that AhR nuclear translocation

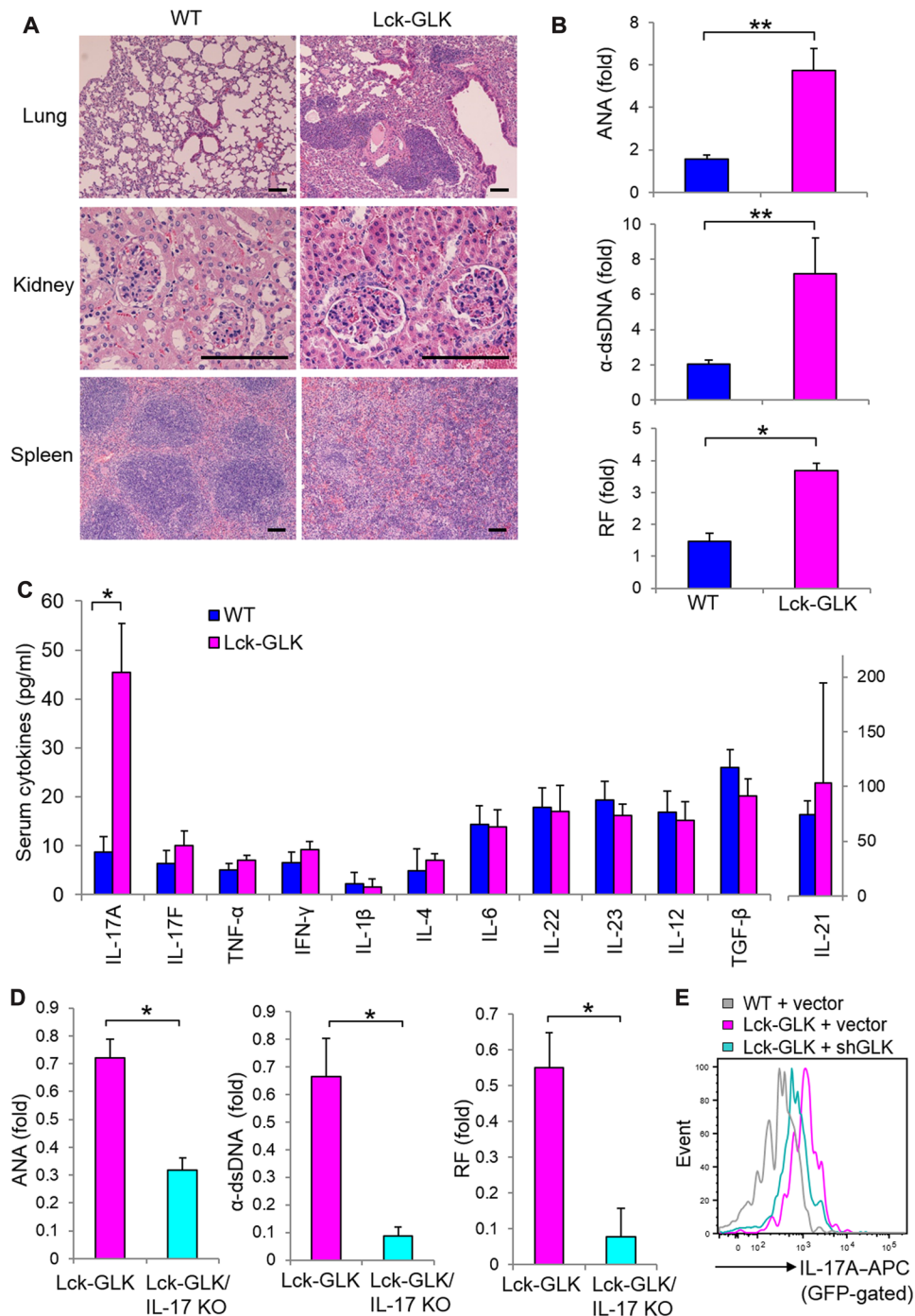


Fig. 1. Lck-GLK Tg mice display autoimmune phenotypes and selectively increased serum IL-17A levels. (A) Hematoxylin and eosin (H&E)-stained sections of the indicated organs from 16-week-old mice. Scale bars, 100 μ m. (B) Levels of serum autoantibodies from 20-week-old mice were determined by ELISAs. The levels are presented relative to the value from one of the wild-type (WT) mice. WT, $n = 7$; Lck-GLK, $n = 8$. (C) The serum levels of cytokines in 4-week-old mice were determined by ELISAs. WT, $n = 20$; Lck-GLK, $n = 16$. (D) The serum levels of autoantibodies in 20-week-old Lck-GLK and Lck-GLK/IL-17A KO mice were determined by ELISAs. The levels are presented relative to the value from one of the Lck-GLK mice. $n = 6$ per group. (E) IL-17A expression was attenuated by GLK shRNA. Murine primary splenic T cells were transfected with green fluorescent protein (GFP)-human GLK shRNA and a control GFP vector. The transfected T cells were stimulated with anti-mouse CD3 antibodies for 3 hours and then determined by flow cytometry at day 3 after transfection. Data show the events of IL-17A-producing T cells (GFP-gated). WT, wild-type littermate controls; Lck-GLK, T cell-specific GLK Tg mice; Lck-GLK/IL-17A KO, Lck-GLK/IL-17A-deficient mice; ANA, antinuclear antibody; α -double-stranded DNA (dsDNA), anti-dsDNA antibody; RF, rheumatoid factor; APC, allophycocyanin. Data shown are representative of three independent experiments. * $P < 0.05$, ** $P < 0.01$ (two-tailed Student's t test).

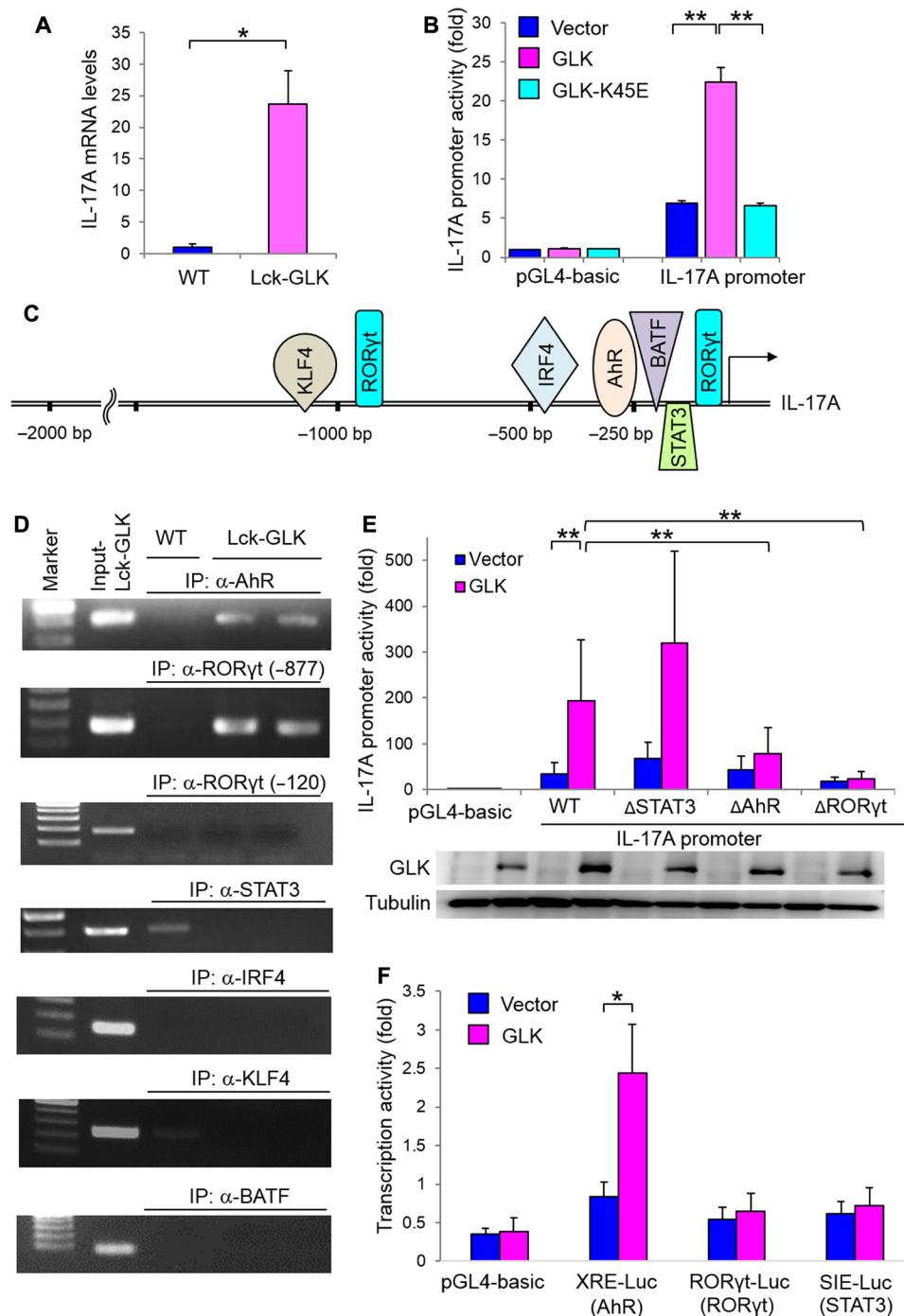


Fig. 2. GLK enhances IL-17A expression by inducing AhR and RORγt. (A) Murine IL-17A mRNA levels in peripheral blood T cells from mice were analyzed by real-time polymerase chain reaction (PCR). The expression levels of IL-17A were normalized to Mrpl32 levels. The fold changes are presented relative to the value of WT mice. Means \pm SEM are shown. $n = 4$ per group. (B) Luciferase reporter activity of the IL-17A promoter. Jurkat T cells were cotransfected with the plasmid encoding GLK or GLK kinase-dead (GLK-K45E) mutant plus the IL-17A promoter (2 kb) construct. Means \pm SEM are shown. (C) Schematic diagram of transcription factors on the IL-17A promoter. bp, base pair. (D) The binding of AhR, RORγt, STAT3, IRF4, KLF4, or BATF to the IL-17A promoter in T cells from mice was analyzed by chromatin immunoprecipitation (IP) (ChIP)-PCR using immunocomplexes from individual IP experiments. (E) Luciferase reporter activity of the IL-17A mutant promoters. Jurkat T cells were cotransfected with empty vector or GLK plasmid plus the IL-17A promoter construct containing a mutated binding element for AhR, RORγt (-877), or STAT3. (F) Luciferase reporter activity of AhR, RORγt (-877), and STAT3 response element (XRE-Luc, RORγt-Luc, and SIE-Luc) in Jurkat T cells cotransfected with empty vector or plasmid encoding GLK. XRE, xenobiotic response element; SIE, sis-inducible element. WT, wild-type littermate controls; Lck-GLK, T cell-specific GLK Tg mice. Data shown are representative of three independent experiments. Means \pm SEM of three independent experiments are shown (B, E, and F). * $P < 0.05$, ** $P < 0.01$ (two-tailed Student's t test).

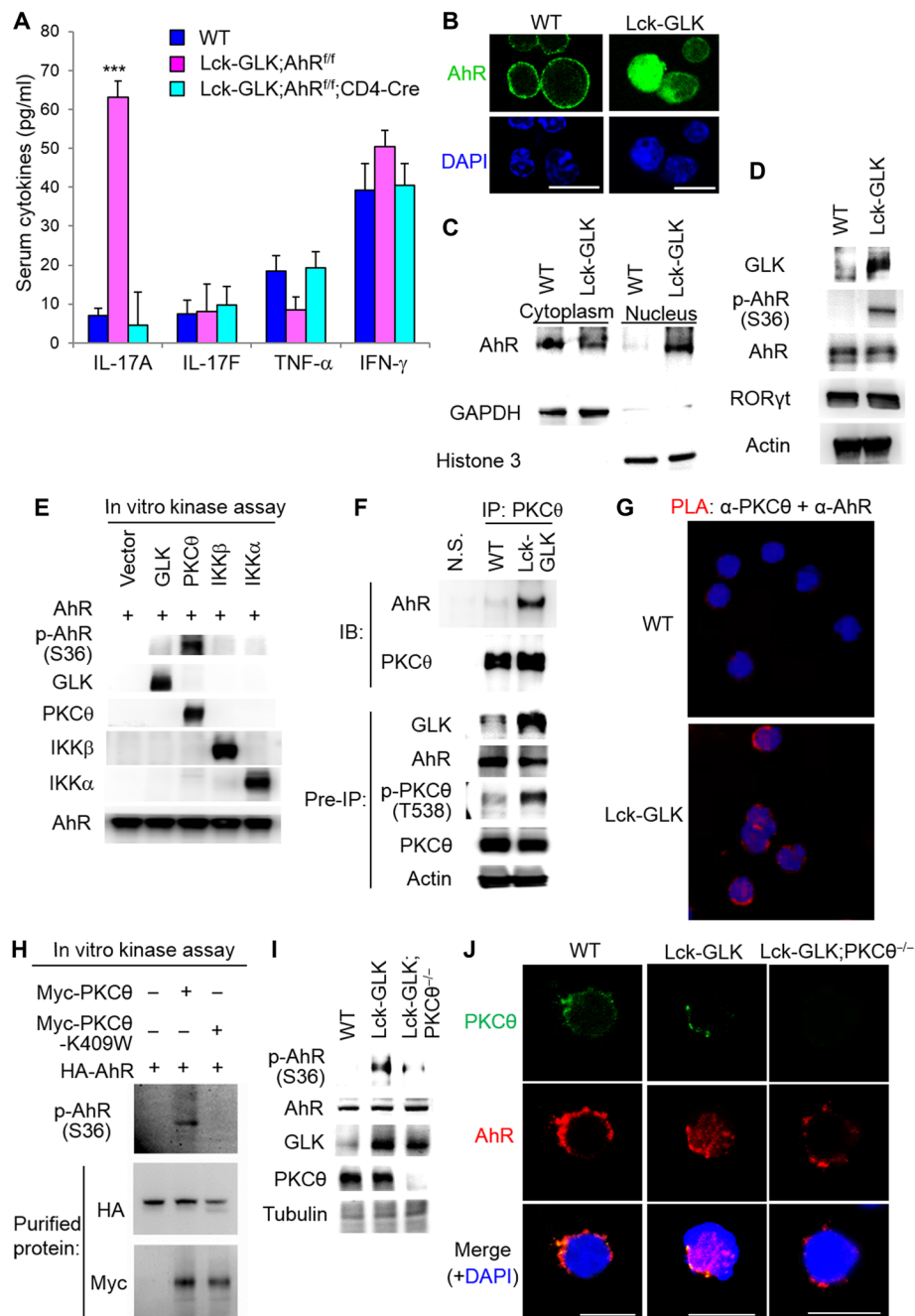


Fig. 3. PKCθ phosphorylates AhR and induces its nuclear translocation. (A) The serum levels of cytokines from 4-week-old WT, Lck-GLK Tg, and Lck-GLK Tg/AhR cKO mice were determined by ELISAs. $n = 8$ per group. Means \pm SEM are shown. WT, wild-type littermate controls; Lck-GLK, T cell-specific GLK Tg mice; Lck-GLK;AhR^{fl/fl};CD4-Cre, T cell-specific GLK Tg mice bred with AhR cKO mice. $***P < 0.001$ (two-tailed Student's t test). (B) Confocal microscopy analysis of subcellular localization of AhR in murine splenic T cells without stimulation. An anti-AhR antibody (clone RPT9, Abcam) was used. Original magnification, $\times 630$; scale bars, 10 μ m. (C) Immunoblotting analyses of AhR, glyceraldehyde-3-phosphate dehydrogenase (GAPDH), and histone 3 in cytoplasmic and nuclear fractions of primary splenic T cells from WT and Lck-GLK Tg mice. (D) Immunoblotting analysis of p-AhR (Ser³⁶), AhR, and GLK in primary splenic T cells of WT and Lck-GLK Tg mice. (E) Immunoblotting analysis of AhR phosphorylation and indicated kinases in in vitro kinase assays using Flag-GLK, Flag-PKCθ, Flag-IKKβ, Flag-IKKα, and hemagglutinin (HA)-AhR (as the substrate) isolated from individually transfected HEK293T cells. (F) Coimmunoprecipitation of endogenous AhR with PKCθ from lysates of primary splenic T cells from WT and Lck-GLK mice without stimulation. N.S., normal serum. (G) Proximity ligation assays (PLAs) of interaction between endogenous PKCθ and AhR in peripheral blood T cells from WT or Lck-GLK Tg mice. Each red dot represents a direct interaction. T cell nucleus was stained with 4',6-diamidino-2-phenylindole (DAPI) (blue). Images were captured with $\times 400$ original magnification by a Leica DM2500 fluorescence microscope. (H) In vitro kinase assays of purified HA-tagged AhR plus either Myc-tagged PKCθ WT or PKCθ kinase-dead (K409W) mutant proteins. (I) Immunoblotting analysis of phosphorylated AhR (Ser³⁶), AhR, GLK, and PKCθ in primary splenic T cells of WT, Lck-GLK Tg, and Lck-GLK Tg mice bred with PKCθ KO mice. (J) Confocal microscopy analysis of subcellular localization of AhR and PKCθ in primary splenic T cells of indicated mice. Original magnification, $\times 630$; scale bars, 10 μ m. WT, wild-type littermate controls; Lck-GLK, T cell-specific GLK Tg mice; Lck-GLK;PKCθ^{-/-}, Lck-GLK Tg mice bred with PKCθ KO mice. Data shown are representative of three independent experiments.

was enhanced in T cells of Lck-GLK Tg mice. In addition, we examined whether GLK signaling induces AhR nuclear translocation by enhancing phosphorylation of AhR. There is only one commercial anti-phospho-AhR antibody that detects phospho-Ser³⁶ AhR; however, the role of Ser³⁶ phosphorylation in AhR nuclear translocation has not been demonstrated (29). Immunoblotting analyses using the anti-phospho-AhR antibody for AhR phosphorylation showed that AhR Ser³⁶ phosphorylation was enhanced in T cells of Lck-GLK Tg mice, as well as in anti-CD3-stimulated T cells (Fig. 3D and fig. S5D). These data suggest that GLK overexpression (and TCR signaling) may induce AhR activity by enhancing AhR Ser³⁶ phosphorylation and nuclear translocation in T cells.

Next, we investigated which kinase is responsible for phosphorylation and nuclear translocation of AhR in T cells of GLK Tg mice. SGK1 (serum/glucocorticoid-regulated kinase 1) can stabilize T_H17 population (30). The basal or TCR-induced SGK1 activation was unchanged in Lck-GLK T cells (fig. S5D), suggesting that SGK1 is not involved in GLK-induced AhR phosphorylation. GLK signaling in T cells induces kinase activities of PKC θ , IKK α , and IKK β (24). To determine which kinase phosphorylates AhR, we immunoprecipitated GLK, PKC θ , IKK α , IKK β , and AhR each from individually transfected human embryonic kidney (HEK) 293T cells and subjected them to *in vitro* kinase assays. The data showed that AhR Ser³⁶ phosphorylation was drastically induced by PKC θ *in vitro* (Fig. 3E). We confirmed the specificity of the antibody for AhR Ser³⁶ phosphorylation using a wild-type AhR or an S36A mutant transfectant by immunoblotting (fig. S5E). Immunofluorescence and confocal imaging analyses showed that PKC θ overexpression enhanced AhR nuclear translocation in Jurkat T cells (fig. S5F) and HEK293T cells (fig. S5G), whereas AhR-S36A mutation stayed in the cytoplasm even in PKC θ -overexpressing cells (fig. S5, F and G). The data indicate that PKC θ -mediated Ser³⁶ phosphorylation of AhR stimulates AhR nuclear translocation. The interaction between PKC θ and AhR was induced in purified T cells of Lck-GLK Tg mice (Fig. 3F). Moreover, the protein-protein interaction/ α (amplified luminescent proximity homogeneous assay) technology assays showed an interaction (<200 nm) between PKC θ and AhR, but not between GLK and AhR (fig. S6A). Furthermore, the fluorescence resonance energy transfer (FRET) analysis showed a direct interaction (1 to 10 nm) between PKC θ and AhR in PKC θ /AhR-cotransfected Jurkat T cells (fig. S6B). To study the subcellular localization and protein interaction (<40 nm) *in vivo*, we performed *in situ* PLA using probes corresponding to PKC θ and AhR. The PLA data showed strong signals in the cytoplasm of T cells from Lck-GLK Tg mice (Fig. 3G and fig. S6C). *In situ* PLA using probes corresponding to Myc and Flag tags showed similar results in Myc-PKC θ - and Flag-AhR-overexpressing HEK293T cells (fig. S6D). *In vitro* binding assays with purified PKC θ and AhR proteins further confirmed this direct interaction (fig. S6E). Furthermore, purified PKC θ phosphorylated AhR at Ser³⁶, whereas purified kinase-dead (K409W) mutant of PKC θ did not (Fig. 3H). These data demonstrate that PKC θ directly interacts with and phosphorylates AhR at Ser³⁶, leading to AhR nuclear translocation.

To verify the role of PKC θ in AhR nuclear translocation and its *in vivo* function, we generated PKC θ KO mice using transcription activator-like effector nuclease (TALEN) technology (fig. S7, A to C). We then bred Lck-GLK Tg mice with PKC θ KO mice to generate Lck-GLK;PKC θ ^{-/-} mice. As expected, PKC θ KO abolished GLK-

induced AhR Ser³⁶ phosphorylation in T cells (Fig. 3I). Immunofluorescence and confocal imaging analyses showed that AhR was detected abundantly in the nucleus of T cells from Lck-GLK Tg mice (Fig. 3J). In contrast, AhR expression was detected in the cytoplasm, but not in the nucleus, of T cells from wild-type and Lck-GLK Tg/PKC θ KO (Lck-GLK;PKC θ ^{-/-}) mice (Fig. 3J). The serum levels of IL-17A and autoantibodies were significantly decreased in Lck-GLK;PKC θ ^{-/-} mice compared to those in Lck-GLK Tg mice (fig. S7, D and E). Moreover, the inflammatory phenotypes were abolished in Lck-GLK Tg/PKC θ KO mice (fig. S7F). Together, these results indicate that GLK induces IL-17A production by activating PKC θ -AhR signaling in T cells.

AhR interacts with ROR γ t and transports ROR γ t into the nucleus

Paradoxically, both AhR- and ROR γ t-binding elements are required for the GLK-induced IL-17A reporter activity (Fig. 2E); however, GLK induced the activity of AhR, but not ROR γ t, response element (Fig. 2F). We suspected that AhR may facilitate induction of ROR γ t activity. We first studied whether GLK induces ROR γ t binding to the IL-17A promoter through AhR. ChIP data showed that the GLK-induced ROR γ t binding to the IL-17A promoter was abolished in AhR KO T cells (Fig. 4A). The data suggest that AhR facilitates the binding of ROR γ t to the IL-17A promoter. Next, we studied whether AhR interacts with ROR γ t. The interaction between endogenous AhR and ROR γ t was drastically enhanced in T cells of Lck-GLK Tg mice (Fig. 4B). Confocal imaging analysis showed colocalization of AhR and ROR γ t in the nucleus of T cells from Lck-GLK Tg mice (Fig. 4C). ChIP analysis using an anti-ROR γ t antibody also showed the binding of ROR γ t to the AhR-binding element of the IL-17A promoter in T cells of Lck-GLK mice (Fig. 4D), suggesting that ROR γ t binds to the AhR-binding element through the AhR-ROR γ t complex formation. Moreover, *in situ* PLA with probes corresponding to AhR and ROR γ t showed strong interaction signals in the nucleus of T cells from Lck-GLK Tg mice compared to those from wild-type mice (Fig. 4E). These data indicate direct interaction between AhR and ROR γ t in the nucleus of T cells from Lck-GLK Tg mice. In addition, similar to AhR nuclear translocation, GLK-induced ROR γ t nuclear translocation was abolished by PKC θ KO (Fig. 4C). The data support the idea that PKC θ -phosphorylated AhR recruits ROR γ t into the nucleus. AhR-mediated ROR γ t nuclear translocation is further confirmed by AhR KO; ROR γ t localized exclusively in the cytoplasm in T cells of Lck-GLK;AhR^{fl/fl};CD4-Cre mice even in the presence of functional PKC θ (Fig. 4C, bottom). Thus, this result rules out the possibility that PKC θ directly regulates ROR γ t nuclear translocation. Collectively, these results indicate that AhR directly interacts with and transports ROR γ t into the nucleus in GLK-overexpressing T cells.

IKK β -mediated ROR γ t Ser⁴⁸⁹ phosphorylation induces AhR-ROR γ t interaction

Surprisingly, *in situ* PLA showed an interaction between AhR and ROR γ t even in the cytoplasm of Lck-GLK;PKC θ ^{-/-} T cells (Fig. 4E). This result suggests that the interaction between AhR and ROR γ t is not regulated by AhR phosphorylation. Interaction between AhR and ROR γ t is still detectable in Lck-GLK;PKC θ ^{-/-} T cells (Fig. 4E); this result may be due to a compensatory signaling event in PKC θ KO mice. To identify the kinase that stimulates the interaction between AhR and ROR γ t, we initially tested the potential role of GLK,

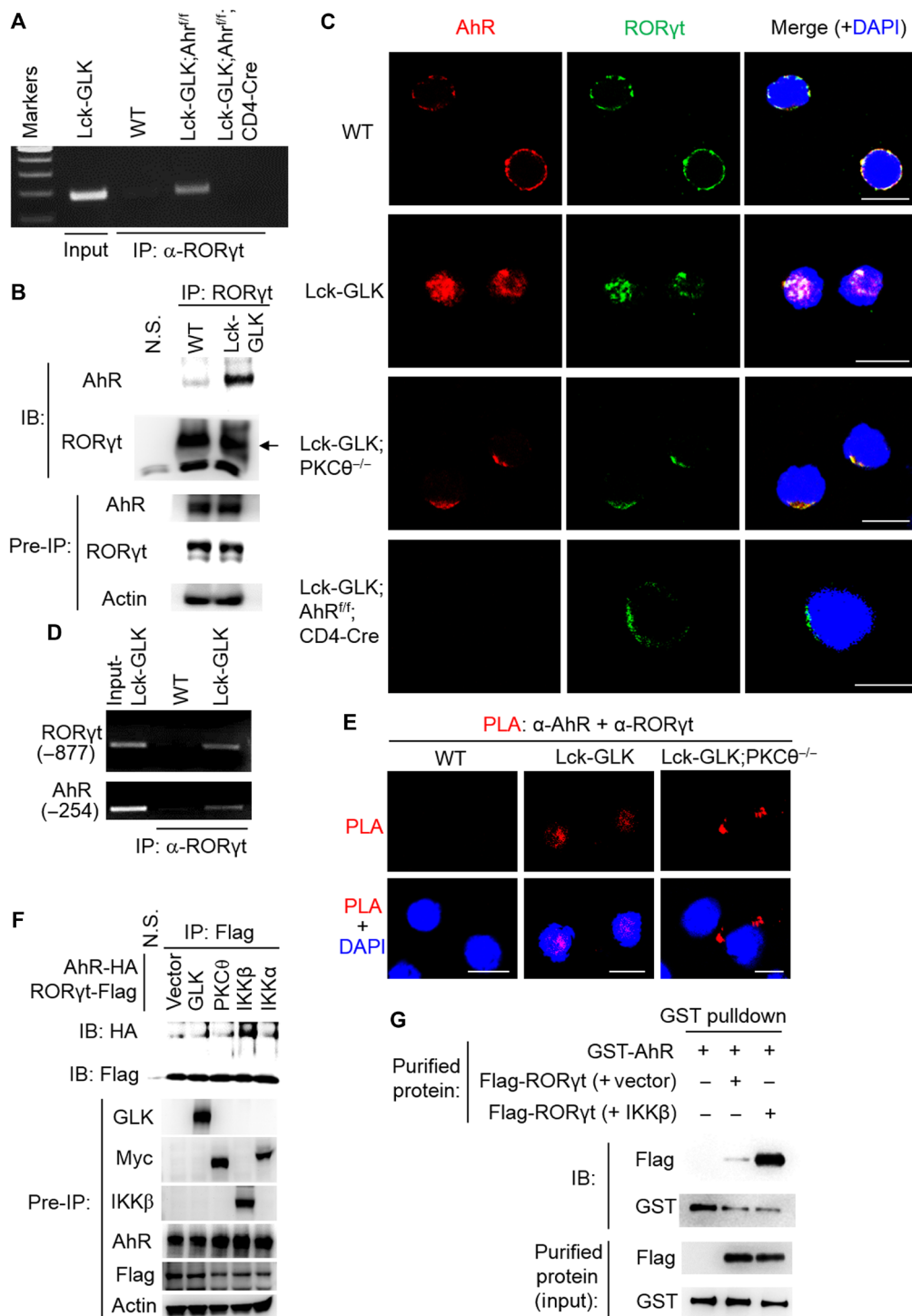


Fig. 4. GLK induces RORγt binding to the IL-17A promoter through AhR and RORγt interaction. (A) Binding of RORγt to the IL-17A promoter in T cells from indicated mice was analyzed by ChIP-PCR. (B) Coimmunoprecipitation of endogenous AhR with RORγt using lysates of primary splenic T cells from WT and Lck-GLK mice without any stimulation. IB, immunoblotting. (C) Confocal microscopy analysis of subcellular localization of AhR and RORγt in primary T cells of WT, Lck-GLK Tg, Lck-GLK;PKCθ^{-/-}, and Lck-GLK;AhR^{fl/fl};CD4-Cre mice. Original magnification, ×630; scale bars, 10 μm. (D) Binding of AhR and RORγt to the IL-17A promoter in T cells from mice was analyzed by ChIP-PCR using anti-RORγt immunocomplexes. (E) Confocal microscopy analysis of PLAs for the interaction between endogenous AhR and RORγt in peripheral blood T cells from WT, Lck-GLK Tg, and Lck-GLK;PKCθ^{-/-} mice. Original magnification, ×630; scale bars, 10 μm. (F) Coimmunoprecipitation experiments of HA-tagged AhR and Flag-tagged RORγt using lysates of HEK293T cells cotransfected with GLK–cyan fluorescent protein (CFP), PKCθ–Myc, IKKβ–CFP, or IKKα–Myc plasmid. (G) GST pull-down assays of purified Flag-tagged RORγt and GST-tagged AhR proteins. Flag-tagged RORγt proteins were eluted with Flag peptides using lysates of HEK293T cells cotransfected with Flag-RORγt plus either CFP–IKKβ or vector. For PLA, each red dot represents a direct interaction. T cell nucleus was stained with DAPI (blue). Data shown are representative of three independent experiments.

IKK α , or IKK β in the induction of AhR-ROR γ t interaction. We cotransfected the kinase GLK, PKC θ , IKK α , or IKK β with AhR plus ROR γ t into HEK293T cells, followed by coimmunoprecipitation assays. The data showed that IKK β overexpression enhanced the interaction between AhR and ROR γ t, whereas overexpression of GLK, PKC θ , and IKK α did not (Fig. 4F). Next, we tested whether IKK β stimulates ROR γ t phosphorylation, which then induces the interaction of ROR γ t with AhR. Flag-tagged ROR γ t was purified from HEK293T cells cotransfected with ROR γ t plus either IKK β or vector. Glutathione S-transferase (GST) pull-down assays showed that purified GST-tagged AhR recombinant proteins strongly interacted with the purified ROR γ t proteins from ROR γ t plus IKK β -cotransfected cells (Fig. 4G). The data suggest that IKK β stimulates a direct interaction between AhR and ROR γ t by inducing ROR γ t phosphorylation. Conversely, PLA data showed that IKK β KO abolished the GLK-induced interaction between AhR and ROR γ t in T cells of Lck-GLK Tg mice (Fig. 5A). In addition, confocal imaging analysis showed that IKK β KO specifically abolished nuclear translocation of ROR γ t, but not AhR, in GLK Tg T cells (Fig. 5B). Consistently, serum IL-17A levels were also decreased in Lck-GLK;IKK β ^{fl/fl};CD4-Cre mice compared to those in Lck-GLK Tg mice (Fig. 5C). Next, we studied whether IKK β interacts directly with ROR γ t. GST and His pull-down assays using purified recombinant GST-tagged IKK β and His-tagged ROR γ t proteins showed a direct interaction between IKK β and ROR γ t (Fig. 5D).

To probe whether IKK β phosphorylates ROR γ t, we individually immunoprecipitated Flag-tagged ROR γ t, IKK β , and IKK β kinase-dead (K44M) mutant from HEK293T transfectants and then subjected them to *in vitro* kinase assays. The data showed that IKK β , but not IKK β -K44M mutant, induced ROR γ t phosphorylation *in vitro* (Fig. 5E). To identify the IKK β -targeted ROR γ t phosphorylation site, we isolated *in vitro* phosphorylated Flag-tagged ROR γ t, followed by mass spectrometry (MS) analyses. Ser⁴⁸⁹ was identified as the ROR γ t phosphorylation site by IKK β (Fig. 5F). To demonstrate phosphorylation of the ROR γ t Ser⁴⁸⁹ site, we generated an anti-phospho-ROR γ t (Ser⁴⁸⁹) antibody, which specifically recognized ROR γ t wild type but not S489A mutant when cotransfected with IKK β (Fig. 5G). Immunoblotting using this phospho-antibody showed that ROR γ t Ser⁴⁸⁹ phosphorylation was induced in T cells of Lck-GLK Tg mice, and the phosphorylation was abolished by IKK β KO (Fig. 5H). Consistently, ROR γ t-S489A mutant failed to interact with AhR under IKK β overexpression (Fig. 5I). Together, in GLK-overexpressing T cells, IKK β phosphorylates ROR γ t at Ser⁴⁸⁹ and induces its interaction with AhR, which then transports ROR γ t into the nucleus and cooperates with ROR γ t to stimulate IL-17A transcription.

Phosphorylated ROR γ t interacts with AhR in TCR-induced or murine autoimmune T cells

Because both GLK and IKK β (24) activation and IL-17A production (31, 32) are inducible by TCR signaling, we asked whether phosphorylated ROR γ t-mediated AhR-ROR γ t interaction is also induced by TCR signaling. We found that, following IKK β activation, anti-CD3 stimulation induced ROR γ t Ser⁴⁸⁹ phosphorylation in murine T cells (Fig. 6A). Moreover, coimmunoprecipitation assays and PLA showed that TCR signaling induced the interaction between endogenous ROR γ t and AhR (Fig. 6B and fig. S8A). TCR signaling also stimulated the interaction between AhR and Ser⁴⁸⁹-phosphorylated ROR γ t (fig. S8B). Conversely, IKK β cKO

abolished the TCR-induced ROR γ t Ser⁴⁸⁹ phosphorylation (Fig. 6C) and the AhR-ROR γ t interaction (Fig. 6D) in T cells. These data suggest that IKK β -mediated ROR γ t phosphorylation and subsequent AhR-ROR γ t interaction are induced during T cell activation. To investigate whether IKK β -mediated ROR γ t phosphorylation regulates IL-17A production after TCR stimulation, we determined secreted cytokines from anti-CD3-stimulated T cells by ELISA. Consistent with previous reports (31, 32), TCR signaling induced IL-17A production in T cells (Fig. 6, E and F). IKK β cKO abolished TCR-induced IL-17A production in T cells (Fig. 6E), supporting the notion that TCR-activated IKK β induces IL-17A production in normal T cells. As expected, TCR-induced levels of several IKK β /NF- κ B-mediated cytokines (IL-2, IFN- γ , IL-4, IL-6, and TNF- α) (table S1) were also reduced in T cells of IKK β cKO mice (Fig. 6E). To further verify the IKK β -ROR γ t-IL-17A pathway, we used primary splenic T cells from T cell-specific ROR γ t cKO mice. Unlike IKK β cKO, ROR γ t cKO only abolished IL-17A production upon TCR stimulation (Fig. 6F). We verified the abolishment of ROR γ t expression in T cells of ROR γ t cKO mice by immunoblotting analysis (Fig. 6G). The data suggest that IKK β -ROR γ t activation mainly induces IL-17A production during TCR signaling, while IKK β -NF- κ B activation regulates the production of multiple cytokines, including IL-2, IFN- γ , IL-4, IL-6, and TNF- α (Fig. 6H and fig. S9).

DISCUSSION

IL-17A is a major proinflammatory cytokine enhanced in the sera of patients with autoimmune diseases. Identification of upstream kinases and transcriptional mechanisms for IL-17A production should facilitate development of novel therapeutic approaches for IL-17A-mediated diseases. Here, we report that GLK, PKC θ , and IKK β are key kinases controlling IL-17A transcription through a bifurcate signaling cascade in pathogenic T_H17 cells.

A key finding of this report indicates that ROR γ t is a novel target of IKK β ; IKK β directly phosphorylates ROR γ t at Ser⁴⁸⁹, leading to IL-17A induction. To our knowledge, this IKK β -phosphorylated Ser⁴⁸⁹ is the first identified pathogenic phosphorylation site of ROR γ t. IL-17A induction is concomitant with increased ROR γ t mRNA levels under T_H17 polarization conditions *in vitro* (28, 33, 34); however, ROR γ t mRNA levels are unchanged during TCR-induced IL-17A induction (32). Because of the strong induction of ROR γ t expression during *in vitro* T_H17 differentiation (28, 33, 34), one might think that ROR γ t proteins are not expressed before T_H17 differentiation. However, ROR γ t mRNA levels in murine T_H0 cells are detectable, although very low (35, 36). Moreover, ROR γ t proteins in human T_H0 cells (36) or murine naive CD4⁺ T cells (37–39) are detectable by immunoblotting. The ROR γ t protein levels in naive CD4⁺ T cells are one-fifth of those in T_H17 cells (38). Furthermore, data using ROR γ t-GFP reporter mice and flow cytometry also show that some CD3⁺ T cells in the spleen, lymph nodes, bone marrow, lung, and skin express ROR γ t proteins (40), and less than 50% of these infiltrating ROR γ t⁺ T cells express IL-17A (40). These data indicate that ROR γ t proteins are expressed in naive T cells. Collectively, either overexpression or Ser⁴⁸⁹ phosphorylation of ROR γ t can lead to IL-17A transcriptional activation. Ser⁴⁸⁹-phosphorylated ROR γ t interacts with AhR and is transported into the nucleus by AhR. Notably, both TCR-stimulated or autoimmune T cells displayed induction of ROR γ t Ser⁴⁸⁹ phosphorylation and AhR-ROR γ t

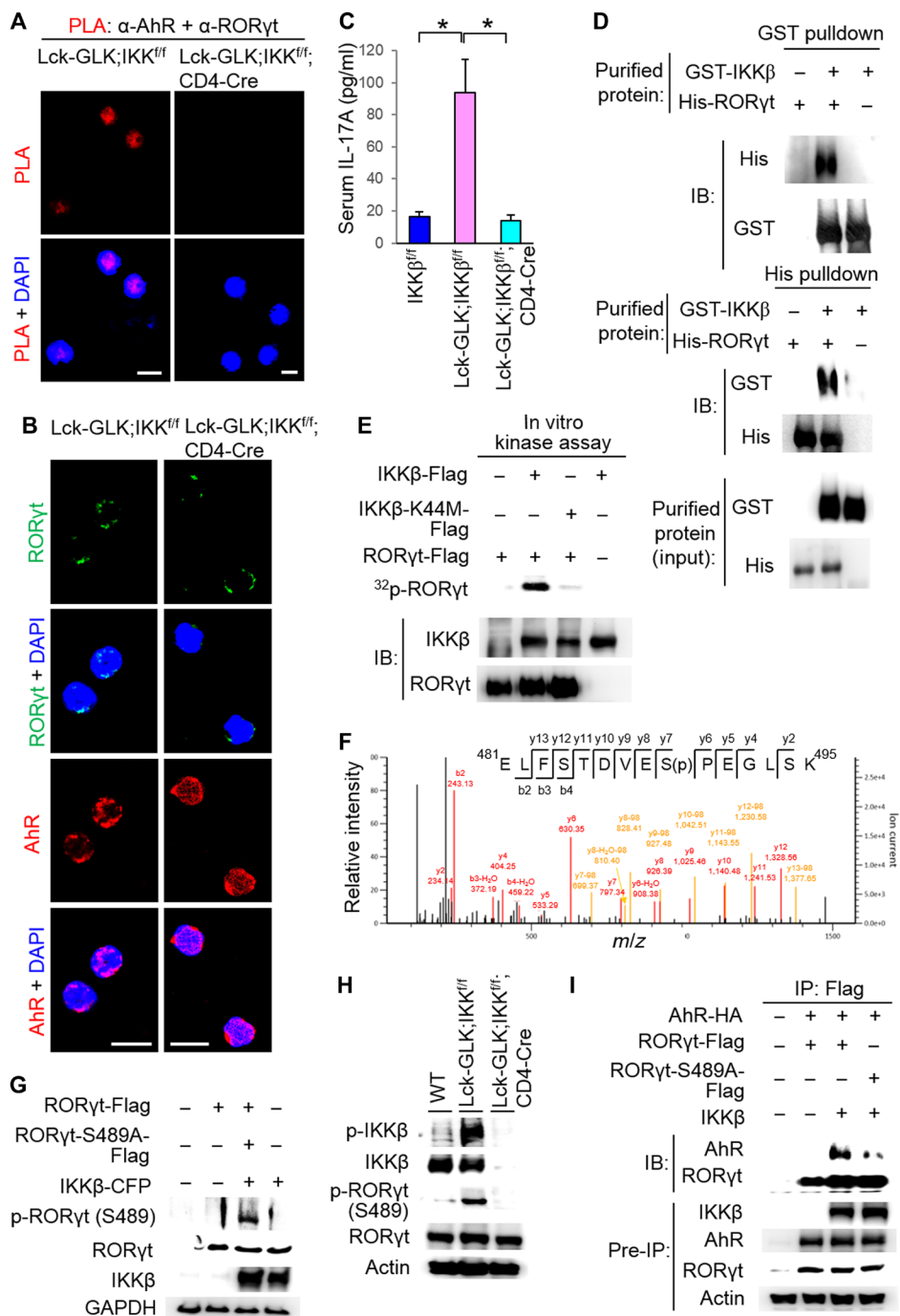


Fig. 5. IKK β phosphorylates ROR γ t Ser⁴⁸⁹, leading to ROR γ t binding to AhR. (A) Confocal microscopy analysis of PLAs for the interaction between endogenous AhR and ROR γ t in peripheral blood T cells from WT, Lck-GLK Tg, and Lck-GLK;IKK^{fl/fl};CD4-Cre mice. (B) Confocal microscopy analysis of subcellular localization of AhR and ROR γ t in primary splenic T cells of WT, Lck-GLK Tg, and Lck-GLK;IKK^{fl/fl};CD4-Cre mice. Original magnification, $\times 630$; scale bars, 10 μ m. (C) The serum levels of cytokines in 8-week-old mice were determined by ELISAs. IKK^{fl/fl}, $n = 6$; Lck-GLK, $n = 6$; Lck-GLK; IKK^{fl/fl}, $n = 5$. Means \pm SEM are shown. * $P < 0.05$ (two-tailed Student's t test). (D) Direct interaction between recombinant proteins of ROR γ t and IKK β . GST or His pull-down assays of purified His-tagged ROR γ t and GST-tagged IKK β proteins. (E) In vitro kinase assays of immunoprecipitated Flag-tagged ROR γ t and either IKK β or IKK β kinase-dead (K44M) mutant proteins from individual HEK293T transfectants. (F) Tandem MS (MS/MS) fragmentation spectra of the tryptic peptides of ROR γ t contain the phosphorylation of Ser⁴⁸⁹. m/z , mass/charge ratio. (G) Antibody specificity of anti-phospho-ROR γ t (Ser⁴⁸⁹) was demonstrated by immunoblotting using HEK293T cells cotransfected with CFP-tagged IKK β plus either Flag-tagged ROR γ t WT or ROR γ t-S489A mutant. (H) Immunoblotting analyses of p-ROR γ t (Ser⁴⁸⁹), ROR γ t, p-IKK β (Ser^{180/181}), and IKK β in primary splenic T cells of WT, Lck-GLK Tg, and Lck-GLK;IKK^{fl/fl}; CD4-Cre mice. (I) Coimmunoprecipitation experiments of HA-tagged AhR and either Flag-tagged ROR γ t WT or ROR γ t-S489A mutant using lysates of HEK293T cells cotransfected with vector or IKK β -CFP plasmid. WT, wild-type littermate controls; Lck-GLK, T cell-specific GLK Tg mice; Lck-GLK;IKK^{fl/fl};CD4-Cre, T cell-specific GLK Tg mice bred with IKK β cKO mice. For PLA, each red dot represents a direct interaction. T cell nucleus was stained with DAPI (blue). Data shown (A, B, D, E, and G to I) are representative of three independent experiments.

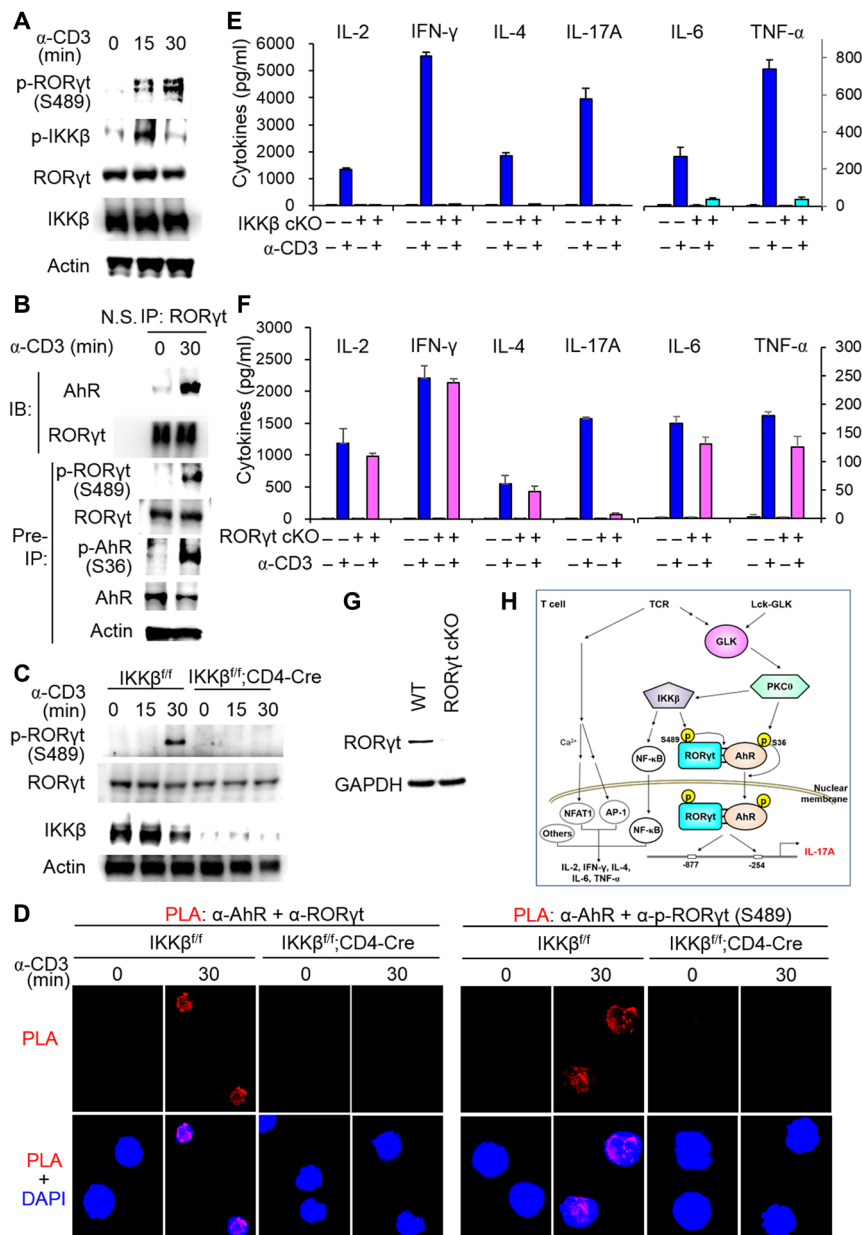


Fig. 6. TCR signaling induces RORyt phosphorylation and subsequent AhR-RORyt interaction. (A) Immunoblotting analysis of p-RORyt (Ser⁴⁸⁹), RORyt, p-IKKβ (Ser^{180/181}), and IKKβ in primary splenic T cells. T cells were stimulated with anti-CD3 antibodies plus streptavidin (3 μg each per milliliter). (B) Coimmunoprecipitation of endogenous AhR with RORyt from lysates of murine primary splenic T cells stimulated with anti-CD3 antibodies plus streptavidin (3 μg each per milliliter). (C) Immunoblotting analysis of p-RORyt (Ser⁴⁸⁹), RORyt, and IKKβ in primary splenic T cells of IKKβ^{fl/fl} or CD4-Cre;IKKβ^{fl/fl} mice. T cells were stimulated with anti-CD3 antibodies plus streptavidin (3 μg each per milliliter). (D) Confocal microscopy analysis of PLAs for the interaction between endogenous AhR and RORyt (left) or between AhR and Ser⁴⁸⁹-phosphorylated RORyt (right) in primary T cells of IKKβ^{fl/fl} or IKKβ^{fl/fl};CD4-Cre mice. T cells were stimulated as in (C). Each red dot represents a direct interaction. T cell nucleus was stained with DAPI (blue). Original magnification, ×630; scale bars, 10 μm. (E and F) ELISA of various cytokines in supernatants of primary splenic T cells from IKKβ^{fl/fl} or IKKβ^{fl/fl};CD4-Cre mice (E), as well as RORyt^{fl/fl} or RORyt^{fl/fl};CD4-Cre mice (F). T cells were stimulated with plate-bound anti-CD3 antibodies (2 μg each per milliliter) for 3 days. Means ± SD are shown. *n* = 3 per group. (G) Immunoblotting of RORyt and GAPDH proteins from primary splenic T cells of RORyt^{fl/fl} or RORyt^{fl/fl};CD4-Cre mice. Data shown (A to G) are representative of three independent experiments. (H) Schematic model of IL-17A transcription induced by the AhR-RORyt complex in GLK-overexpressing or TCR-stimulated T cells. GLK overexpression in T cells of T cell-specific GLK Tg (Lck-GLK Tg) mice induces AhR Ser³⁶ phosphorylation through PKCθ and also induces RORyt Ser⁴⁸⁹ phosphorylation through IKKβ. Once RORyt is phosphorylated, RORyt interacts directly with AhR. Phosphorylated AhR is responsible for transporting RORyt into cell nucleus. The AhR-RORyt complex binds to both the RORyt-binding element (−877 to −872) and the AhR-binding element (−254 to −249) of the IL-17A promoter, leading to induction of IL-17A transcription. In normal T cells, TCR stimulation also induces GLK kinase activity and downstream signaling, including IKKβ activation, RORyt Ser⁴⁸⁹ phosphorylation, and the AhR-RORyt interaction. Besides NF-κB, other critical transcription factors [such as nuclear factor of activated T cell 1 (NFAT1) or activator protein 1 (AP-1)] are also required for the transcriptional activation of IL-2, IFN-γ, IL-4, IL-6, and TNF-α in T cells. “Others” denotes other critical transcription factors (table S1). NF-κB is required for TCR-induced production of multiple cytokines; however, the GLK-IKKβ-NF-κB cascade alone is not sufficient for the induction of multiple cytokines. Collectively, GLK overexpression or TCR signaling induces IL-17A transcription through AhR and RORyt in T cells.

interaction. These findings suggest that IKK β -mediated ROR γ t Ser⁴⁸⁹ phosphorylation is a common transcriptional activation mechanism of IL-17A induction in T cell activation or autoimmune diseases. Ubiquitination of ROR γ t at Lys⁴⁴⁶ negatively regulates IL-17A, but not IL-17F, production by blocking its interaction with the coactivator SRC1 (41). In contrast, ROR γ t K63-linked ubiquitination at Lys⁶⁹ is required for IL-17A transcription (42). In addition, CD5 signaling may contribute to ROR γ t nuclear translocation in T_H17 differentiation in vitro (43). IL-6 plus IL-23 stimulation also induces ROR γ t nuclear translocation in murine neutrophils in vitro (44). Thus, it is likely that ROR γ t Ser⁴⁸⁹ phosphorylation also cross-talks with or is involved in other signaling events.

One of the exciting findings in this report is that AhR is responsible for nuclear translocation of ROR γ t. PKC θ directly activates AhR by phosphorylating AhR at Ser³⁶ during TCR signaling and GLK signaling. Ser³⁶ phosphorylation of AhR mediates the nuclear translocation of the AhR-ROR γ t complex, and both transcription factors then induce IL-17A transcription. Paradoxically, GLK overexpression only enhanced AhR (but not ROR γ t) response element-driven reporter activity. Nevertheless, the mutation of either AhR-binding site or ROR γ t-binding site within the IL-17A promoter blocked GLK signaling-induced IL-17A transcription. It is likely that, besides nuclear translocation of ROR γ t by AhR, the binding of AhR to the AhR response element or indirectly binding to other regions within the IL-17A promoter may also facilitate the binding of ROR γ t to the IL-17A promoter. The binding of AhR with its ligand triggers the nuclear translocation and DNA binding activity of AhR; distinct ligands stimulate different physiological functions of AhR in T cells (45, 46). AhR activation by a natural ligand results in enhanced T_H17 population and severe EAE symptoms in mice (45, 47). Besides TCR signaling, it is possible that AhR Ser³⁶ phosphorylation may also regulate IL-17A production in ligand-induced or other unliganded signaling pathways.

GLK is required for TCR signaling and production of several cytokines such as IFN- γ , IL-4, and IL-2 (24); however, Lck-GLK Tg mice showed selective overproduction of IL-17A, but not other NF- κ B-mediated cytokines. This dichotomy may be attributed to the fact that, besides NF- κ B, other transcription factors (such as NFAT1 or AP-1) are also required for the transcriptional activation of IL-2, IL-4, IFN- γ , IL-6, or TNF- α during TCR signaling (table S1) (48, 49). Thus, activation of NF- κ B alone without activation of other critical transcription factors in T cell is not sufficient to induce the production of IL-2, IL-4, IFN- γ , IL-6, or TNF- α (Fig. 6H). T cell-specific IKK β Tg mice do not display any significant induction of IL-2 or IFN- γ in resting T cells, while basal levels of the T cell activation markers CD25 and CD69 are enhanced (50). Consistently, activated IKK β in GLK Tg T cells is not sufficient to induce NF- κ B-mediated cytokines. In addition, STAT3 activation is required for the transcription of IL-17F, IL-21, IL-22, and IL-23R in T_H17 cells (39, 51–53); conversely, IL-6 or IL-21 induces STAT3 activation in T_H17 cells (39, 51, 53). It is likely that the reason for the lack of IL-17F/IL-21/IL-22 induction and IL-23R overexpression in GLK Tg T cells may be the lack of STAT3 activation. Besides IL-17A, IL-17F and IL-22 are also regulated by ROR γ t (53). However, the Lys⁴⁶⁶-ubiquitinated ROR γ t regulates the production of IL-17A, but not IL-17F (41). Our results in this study showed the binding of the AhR-ROR γ t complex to the –877, but not the –120, region of the IL-17A promoter. These findings suggest that the AhR-ROR γ t complex does not bind to the ROR γ t-binding elements

that regulate the transcription of IL-17F and IL-22. Collectively, the GLK-IKK β -ROR γ t axis is not sufficient to induce multiple cytokines because of the lack of activation of other critical transcription factors or the lack of AhR-ROR γ t complex-binding elements. Last, it is also plausible that GLK overexpression may suppress the production of multiple cytokines through an unknown inhibitory mechanism.

Our study reveals a critical pathogenic mechanism of GLK-induced IL-17A transcription in autoimmune diseases. In summary, GLK signaling induces Ser³⁶ phosphorylation and nuclear translocation of AhR through PKC θ . AhR interacts with ROR γ t and transports ROR γ t into the nucleus of T cells. The GLK-PKC θ -AhR axis is responsible for the nuclear translocation of ROR γ t, but not for the interaction of ROR γ t with AhR. On the other hand, the interaction between ROR γ t and AhR is controlled by IKK β , which phosphorylates ROR γ t at Ser⁴⁸⁹. Similarly, TCR signaling also induces phosphorylation of AhR and ROR γ t, as well as the interaction and nuclear translocation of the AhR-ROR γ t complex. Thus, TCR or GLK signaling induces IL-17A transcription through the novel ROR γ t Ser⁴⁸⁹ phosphorylation and subsequent AhR-ROR γ t interaction/nuclear translocation. Collectively, the GLK-PKC θ /IKK β -AhR/ROR γ t pathway plays a critical role in the pathogenesis of IL-17A-mediated autoimmune diseases (Fig. 6H and fig. S9). This pathway may also be involved in other IL-17A-mediated inflammatory diseases that are induced by other IL-17A⁺ cell types (for example, group 3 innate lymphoid cells). Thus, inhibitors of GLK or the AhR-ROR γ t complex could be used as IL-17A-blocking agents for the treatment of IL-17A-mediated diseases. Furthermore, since GLK overexpression is also correlated with cancer recurrence (54, 55), studying the potential involvement of GLK-IL-17A signaling in cancer recurrence/metastasis may help future development of cancer therapy.

METHODS

Mice

All animal experiments were performed in the Association for Assessment and Accreditation of Laboratory Animal Care International (AAALAC)-accredited animal housing facilities at the National Health Research Institutes (NHRI). All mice were used according to the protocols and guidelines approved by the Institutional Animal Care and Use Committee of NHRI. Floxed AhR mice (JAX 006203), IL-17A-deficient mice (JAX 016879), floxed ROR γ t mice (JAX 008771), and floxed IKK β mice (EMMA 001921) were purchased from the Jackson Laboratory (JAX) or the European Mouse Mutant Archive (EMMA). The three aforementioned mouse lines were backcrossed for 10 generations onto the C57BL/6 background. The data presented in this study were performed on sex-matched, 4- to 26-week-old littermates. For T cell development analyses, 5-week-old, sex-matched mice were used. All mice used in this study were maintained in temperature-controlled and pathogen-free cages.

Generation of Lck-GLK Tg mice and PKC θ KO mice

A full-length human GLK coding sequence was placed downstream of the proximal Lck promoter (fig. S1A). Lck-GLK Tg mice in C57BL/6 background were generated using pronuclear microinjection by NHRI Transgenic Mouse Core. Two independent Lck-GLK Tg mouse lines were used. Lck-GLK Tg mouse line #1 was used in all the Lck-GLK Tg experiments, except for the studies in figs. S1B and S2E, in which Lck-GLK Tg mouse line #2 was used. PKC θ KO mice were generated

by TALEN-mediated gene targeting (fig. S7, A to C); the nucleotides 5'-GGTGGAACTAAAATAATATGTCTTAGAGCCCAT-ACATACAGTGTCTTTGTCATTTTCTAGGGAA-CAACCATGTCACCGTTTC-3' of the PKC θ intron 1 and exon 2 were deleted in the mutated allele. For TALEN-mediated gene targeting in mice, embryo microinjection of TALEN mRNA was performed by NHRI Transgenic Mouse Core.

Cells

Human Jurkat T leukemia cells [American Type Culture Collection (ATCC), TIB-152] were cultured in RPMI 1640 (Invitrogen) containing 10% fetal calf serum (FCS; Invitrogen) plus penicillin (10 U/ml) and streptomycin (10 mg/ml) (Invitrogen). HEK293T cells (ATCC, CRL-11268) were cultured in Dulbecco's modified Eagle's medium (Invitrogen) containing 10% FCS plus penicillin (10 U/ml) and streptomycin (10 mg/ml). All cell lines used were tested and confirmed to be negative for mycoplasma. Primary murine T cells were negatively selected from the spleen, lymph nodes, or peripheral bloods of mice using magnetically coupled antibodies against CD11b, B220, CD49b, CD235, and TER-119 [magnetic cell separation kit (Miltenyi Biotec)]. To induce IL-17A production of 3-day-cultured T cells (Fig. 1E), the primary T cells were stimulated with biotin-conjugated anti-CD3 antibodies (3 μ g/ml) plus streptavidin (3 μ g/ml) for 3 hours at 37°C.

Reagents and antibodies

GLK antibody (α -GLK-N) was generated by immunization of rabbits with peptides (murine GLK epitope: ⁴GFDLSRRNPQEDFELI¹⁹; identical to human GLK protein sequences 4 to 19) and was used for Figs. 2E, 3 (D and E), and 4F. Anti-GLK monoclonal antibody (clone C3) was generated by immunization of mice with peptides (murine GLK epitope: ⁵¹⁴EQRGNTNLSRKEKDVPKPI⁵³³) and was used for Fig. 3 (F and I) and fig. S5D. The antibody for phosphorylated ROR γ t Ser⁴⁸⁹ was generated by immunization of a rabbit with phosphopeptides (murine ROR γ t epitope: ⁴⁸³FSTDVE[pS]PEGLSK⁴⁹⁵). Anti-Myc (clone 9E10), anti-Flag (clone M2), and anti-HA (clone 12CA5) antibodies were purchased from Sigma-Aldrich. Anti-p-AhR (Ser³⁶; #A0765) antibody was purchased from Assay Biotechnology. Anti-AhR (clone RPT9), anti-p-IKK β (Ser^{180/181}; #ab55341), and anti-GAPDH (clone mAbcam 9484, catalog #ab9482) antibodies were purchased from Abcam. Anti-PKC θ (#3551-1) and anti-actin (clone E184) antibodies were purchased from Epitomics. Anti-p-PKC θ (Thr⁵³⁸; #ab63365), anti-p-STAT3 (Tyr⁷⁰⁵; clone D3A7), anti-IKK α (#2682), anti-IKK β (#2678), anti-p-SGK1 (Thr²⁵⁶; #2939), anti-SGK1 (clone D27C11), anti-histone 3 (#9715S), anti-IRF4 (#4964S), and anti-BATF (#8638S) antibodies were purchased from Cell Signaling Technology. Anti-STAT3 (#06-596) and anti-ROR γ t (clone 6F3.1) antibodies were purchased from Millipore. Anti-KLF4 (#AF3158) and anti-IL-23 receptor (#bs-1460) antibodies were purchased from R&D Systems and Bioss Antibodies, respectively.

Plasmids and recombinant proteins

The expression plasmids for GLK and GLK kinase-dead mutant (GLK-K45E) were reported previously (22). CFP-tagged PKC θ , yellow fluorescent protein (YFP)-tagged AhR, Myc-tagged PKC θ , HA-tagged AhR, and Flag-tagged PKC θ plasmids were constructed by subcloning individual complementary DNAs into pCMV6-AC-CFP, pCMV6-AC-YFP, pCMV6-AC-Myc, pCMV6-AC-HA, or pCMV6-AC-Flag vector (OriGene Technologies). HA-tagged AhR-S36A mutant and Myc-tagged PKC θ -K409W (kinase-dead) mutant plasmids were generated by site-directed mutagenesis. GST-

tagged PKC θ and GST-tagged PKC θ -K409W plasmids were also individually constructed by subcloning into pGEX-4T vector. The human GLK shRNA (5'-GTGCCACTTAGAATGTTTGAAA-3') was obtained from the National RNAi Core Facility (Taiwan) and subcloned into pSUPER-GFP vector (Oligoengine). The IL-17A reporter plasmid was a gift from W. Strober (Addgene plasmid #20124) (28). The IL-17A promoter constructs containing a mutated binding element for AhR, ROR γ t (-877), ROR γ t (-120), or STAT3 were generated by site-directed mutagenesis using Fusion DNA polymerase (Thermo Fisher Scientific) according to the manufacturer's protocol. The following primers were used for mutagenesis (mutated binding elements are underlined and italicized; mutated nucleotides are shown in bold font): AhR-binding site (18), 5'-ATGTCCATACATACATGATACTGAATCACAGC-3'; ROR γ t-binding site (-887) (28), 5'-CTCAAAGACATAAAGGCAA***CCGTGAT***TCTCATGGAGAGGAGAG-3'; ROR γ t-binding site (-120), 5'-GGTTCTGTG***CTGCAAT***CATTTGAGG-3' (11); and STAT3-binding site (56), 5'-AGACAGATGTTGC***CTGTCA***TAAAGGGGTGGTT-3'.

The mutant constructs were verified by DNA sequencing. The plasmids pGL4.43-Luc2P-XRE (AhR-response XRE-Luc), pGL4.47-Luc2P-SIE (STAT3-responsive SIE-Luc), pGL4.32-Luc2P-NF- κ B-RE-Hygro, and pGL4 luciferase reporter vector were purchased from Promega. The plasmid for the ROR γ t (-877) response element-driven reporter was constructed by cloning four copies of the ROR γ t (-877) response element into the pGL4.43 luciferase reporter vector. For in vitro binding assays, purified AhR proteins were isolated from HA-AhR-transfected HEK293T cells, followed by HA-peptide elution. Purified recombinant GST-PKC θ and GST-IKK β proteins were purchased from SignalChem. Purified recombinant 6 \times His-ROR γ proteins were purchased from MyBioSource. Recombinant proteins of GST-tagged PKC θ K409W proteins were isolated from *Escherichia coli* (BL21) and then purified by GST pulldown assays. Purified Flag-tagged ROR γ t protein was immunoprecipitated and then eluted with Flag peptides from lysates of HEK293T cells that were cotransfected with Flag-ROR γ t plus either CFP-IKK β or vector. Purified recombinant protein of GST-tagged AhR was purchased from Abnova.

Luciferase reporter assays

The 2-kb IL-17A promoter-driven firefly luciferase reporter plasmid and a *Renilla* luciferase control plasmid (pRL-TK) were cotransfected into Jurkat T cells. After 24 hours, 1 \times 10⁶ cells were harvested, washed with phosphate-buffered saline, and resuspended in 60 μ l of RPMI 1640 plus 60 μ l of lysis buffer. Data represent the mean of the ratios of the firefly luciferase activity to the *Renilla* luciferase activity.

Enzyme-linked immunosorbent assays

Serum levels of IL-1 β , IL-4, IL-6, IL-12, IL-17F, IL-21, IL-22, IL-23, IFN- γ , TNF- α , and TGF- β were analyzed by individual ELISA kits purchased from eBioscience. The IL-17A levels were determined using an ELISA kit from BioLegend. The serum levels of ANAs, anti-dsDNA antibody, and RF were analyzed by ELISA kits purchased from Alpha Diagnostic International.

ALPHA technology

ALPHA technology/protein-protein interaction assays were performed according to the manufacturer's protocol from PerkinElmer Life Sciences, as described in a previous publication (57). When the protein-donor pair was within 200 nm, a luminescent signal was detected by an EnVision 2104 Multilabel Plate Reader (PerkinElmer Life Sciences).

FRET assays

FRET signal in live cells was detected by an EnVision 2104 Multilabel Plate Reader (PerkinElmer Life Sciences). The reaction was excited by light passing through a 430-nm filter (with 8 nm bandwidth), and the intensity of emitted fluorescence passing through a 530-nm filter (with 8 nm bandwidth) was recorded. If the protein-protein pair was in close proximity (1 to 10 nm), a 530-nm signal would be detected. The FRET efficiency was calculated by a formula, $\text{efficiency} = (1 - \text{FDA}/\text{FD}) \times 100\%$ (where FDA is the relative fluorescence intensities of the donor in the presence of the acceptor and FD is the relative fluorescence intensities of the donor in the absence of the acceptor).

In situ PLA

PLAs were performed using the Duolink In Situ Red Starter kit (Sigma-Aldrich) according to the manufacturer's instructions. Briefly, cells were incubated with rabbit or mouse primary antibodies for each molecule pair (AhR plus PKC θ , AhR plus ROR γ t, or Flag plus Myc), followed by species-specific secondary antibodies conjugated with oligonucleotides (PLA probes). After ligation and amplification reactions, the PLA signals from each pair of PLA probes in close proximity (<40 nm) were visualized as individual red dots by a fluorescence microscope (Leica DM2500) or a confocal microscope (Leica TCS SP5 II). Each red dot represents a direct interaction.

ChIP assays

Peripheral blood T cells of mice were cross-linked with 1% formaldehyde for 10 min at room temperature. The lysates were sonicated (3 \times 9 s) on ice to generate 200- to 1000-base pair DNA fragments. The cell extracts were immunoprecipitated with 5 μ g of anti-ROR γ t, anti-AhR, or anti-STAT3 antibodies plus protein G Dynabeads (Invitrogen) for 4 hours at 4°C on a rotating wheel. After washing three times, immunocomplexes were incubated at 94°C for 15 min for reverse cross-linking and then treated with protease K. The DNA fragments were purified using a PCR purification kit (GE Healthcare) and subjected to PCR for 35 cycles. The primers for the IL-17A promoter containing the ROR γ t-binding sites (-877 to -872) (28) and (-120 to -115) (11), AhR-binding site (-254 to -249) (18), STAT3-binding site (-150 to -145) (56), IRF4-binding site (-429 to -421) (14), KLF4-binding site (-1097 to -1083) (16), or BATF (-243 to -176) (15) were as follows: ROR γ t (-877 to -872), 5'-CTGAAGAGCTGGGACCTAATG-3' (forward) and 5'-GACTACTAACAGGAGGAGATG-3' (reverse); ROR γ t (-120 to -115), 5'-GGTTCTGTGCTGACCTCATTGAG-3' (forward) and 5'-CACAGATGAAGCTCTCCCTGG-3' (reverse); AhR, 5'-GAGACTCACAAACCATTACTATG-3' (forward) and 5'-CACAGATGAAGCTCTCCCTGG-3' (reverse); STAT3, 5'-GAGACTCACAAACCATTACTATG-3' (forward) and 5'-CACAGATGAAGCTCTCCCTGG-3' (reverse); IRF4, 5'-GGGCAAGGGATGCTCTCTAG-3' (forward) and 5'-CTGAAGCTGCTGCAGAGCTG-3' (reverse); KLF4, 5'-GGGTATTATCCCAAGGGTATCC-3' (forward) and 5'-ATGCAGCATGAGGTGGACCGAT-3' (reverse); BATF, 5'-GAACTTCTGCCCTTCCCATCT-3' (forward) and 5'-CAGCACAGAACCACCCCTTT-3' (reverse).

Immunoprecipitation, GST/His pull-down, and immunoblotting analyses

Immunoprecipitation was performed by preincubation of 0.5 to 1 mg of protein lysates with 1 μ g of antibody for 1 hour at 4°C, fol-

lowed by the addition of 20 μ l of protein A/G Sepharose beads for 3 hours. For GST and His pull-down assays, GST- and His-tagged proteins plus their interacting proteins were incubated for 3 hours with glutathione Sepharose beads (GE Healthcare) and Ni Sepharose beads (GE Healthcare), respectively. The immunocomplexes or GST/His pull-down complexes were washed with lysis buffer (1.5 mM MgCl₂, 0.2% NP-40, 125 mM NaCl, 5% glycerol, 25 mM NaF, 50 mM Tris-HCl, and 1 mM Na₃VO₄) three times at 4°C, followed by boiling in 5 \times loading buffer at 95°C for 3 min. The immunoblotting analyses were performed as described previously (57).

Cell transfections, T cell stimulation, in vitro kinase assays for PKC θ or IKK β , and flow cytometric analyses

These experiments were performed as described previously (24).

Immunofluorescence and confocal imaging

Cells were fixed in cold methanol for 2 min. After permeation with 0.25% Triton X-100 for 1 hour, the cells were blocked with 5% bovine serum albumin for 2 hours. The cells were incubated with primary antibodies (1:200 dilution) for 24 hours and then with secondary antibodies (1:500 dilution) for 2 hours. The secondary antibodies donkey anti-rabbit immunoglobulin G (IgG)-Alexa Fluor 568 and goat anti-mouse IgG-Alexa Fluor 488 were purchased from Abcam and Life Technologies, respectively. The cover slides were mounted in Fluoroshield with DAPI (GeneTex) and analyzed using a Leica TCS SP5 confocal microscope.

In vitro T cell differentiation assays

CD4⁺ splenic T cells were purified from mice. Cells (5 \times 10⁵) were cultured in 1 ml of RPMI 1640 in 48-well plates coated with anti-CD3 (2 μ g/ml) and anti-CD28 (3 μ g/ml) antibodies. For T_H17 differentiation, splenic CD4⁺ cells were cultured in the medium containing IL-23 recombinant proteins (50 ng/ml; R&D Systems), IL-6 recombinant proteins (20 ng/ml; R&D Systems), TGF- β recombinant proteins (5 ng/ml; R&D Systems), and anti-IL-4 (5 μ g/ml; BioLegend) and anti-IFN- γ (5 μ g/ml; BioLegend) antibodies. For T_H1 differentiation, CD4⁺ splenic cells were cultured in the medium containing IL-12 recombinant proteins (5 ng/ml; R&D Systems) and anti-IL-4 antibodies (1 μ g/ml; BioLegend).

Liquid chromatography-MS

After in vitro kinase assays, protein bands of Flag-tagged ROR γ t were collected from InstantBlue (GeneMark)-stained SDS-polyacrylamide gel electrophoresis gels. Proteins were digested with trypsin and subjected to liquid chromatography-MS/MS analyses by an LTQ Orbitrap Elite hybrid mass spectrometer as described previously (57).

Statistical analyses

All experiments were repeated at least three times. Data are means \pm SEM. The statistical significance between two unpaired groups was analyzed using two-tailed Student's *t* test. *P* values of less than 0.05 were considered statistically significant.

SUPPLEMENTARY MATERIALS

Supplementary material for this article is available at <http://advances.sciencemag.org/cgi/content/full/4/9/eaat5401/DC1>

Fig. S1. Normal T cell and B cell development in Lck-GLK Tg mice.

Fig. S2. Inflammatory phenotypes and enhanced T_H17 differentiation in Lck-GLK Tg mice.

Fig. S3. Autoimmune responses in Lck-GLK Tg mice are abolished by IL-17A deficiency.

Fig. S4. GLK transgene does not regulate IL-23 receptor expression, STAT3 phosphorylation, and ROR γ t-binding element at the \sim 120 region of the IL-17A promoter.

Fig. S5. PKC θ controls Ser³⁶ phosphorylation-mediated AhR nuclear translocation and AhR-mediated autoimmune responses.

Fig. S6. PKC θ directly interacts with AhR in the cytoplasm of Lck-GLK T cells.

Fig. S7. Autoimmune responses in Lck-GLK Tg mice are reduced by PKC θ KO.

Fig. S8. TCR signaling induces in vivo interaction between AhR and ROR γ t.

Fig. S9. Schematic model of AhR/ROR γ t-mediated IL-17A transcription in T cells of Lck-GLK Tg mice with different gene-KO backgrounds.

Table S1. Transcription factors of NF- κ B-mediated cytokines.

References (58, 59)

REFERENCES AND NOTES

- D. D. Patel, V. K. Kuchroo, Th17 cell pathway in human immunity: Lessons from genetics and therapeutic interventions. *Immunity* **43**, 1040–1051 (2015).
- S. L. Gaffen, R. Jain, A. V. Garg, D. J. Cua, The IL-23–IL-17 immune axis: From mechanisms to therapeutic testing. *Nat. Rev. Immunol.* **14**, 585–600 (2014).
- S. Kotake, N. Udagawa, N. Takahashi, K. Matsuzaki, K. Itoh, S. Ishiyama, S. Saito, K. Inoue, N. Kamatani, M. T. Gillespie, T. J. Martin, T. Suda, IL-17 in synovial fluids from patients with rheumatoid arthritis is a potent stimulator of osteoclastogenesis. *J. Clin. Invest.* **103**, 1345–1352 (1999).
- M. Mitsdoerffer, Y. Lee, A. Jäger, H.-J. Kim, T. Korn, J. K. Kolls, H. Cantor, E. Bettelli, V. K. Kuchroo, Proinflammatory T helper type 17 cells are effective B-cell helpers. *Proc. Natl. Acad. Sci. U.S.A.* **107**, 14292–14297 (2010).
- H. Park, Z. Li, X. O. Yang, S. H. Chang, R. Nurieva, Y.-H. Wang, Y. Wang, L. Hood, Z. Zhu, Q. Tian, C. Dong, A distinct lineage of CD4 T cells regulates tissue inflammation by producing interleukin 17. *Nat. Immunol.* **6**, 1133–1141 (2005).
- I. I. Ivanov, L. Zhou, D. R. Littman, Transcriptional regulation of Th17 cell differentiation. *Semin. Immunol.* **19**, 409–417 (2007).
- C. Dong, T_H17 cells in development: An updated view of their molecular identity and genetic programming. *Nat. Rev. Immunol.* **8**, 337–348 (2008).
- X. O. Yang, R. Nurieva, G. J. Martinez, H. S. Kang, Y. Chung, B. P. Pappu, B. Shah, S. H. Chang, K. S. Schluns, S. S. Watowich, X.-H. Feng, A. M. Jetten, C. Dong, Molecular antagonism and plasticity of regulatory and inflammatory T cell programs. *Immunity* **29**, 44–56 (2008).
- I. I. Ivanov, B. S. McKenzie, L. Zhou, C. E. Tadokoro, A. Lepelletier, J. J. Lafaille, D. J. Cua, D. R. Littman, The orphan nuclear receptor ROR γ t directs the differentiation program of proinflammatory IL-17⁺ T helper cells. *Cell* **126**, 1121–1133 (2006).
- L. Zhou, J. E. Lopes, M. M. W. Chong, I. I. Ivanov, R. Min, G. D. Victora, Y. Shen, J. Du, Y. P. Rubtsov, A. Y. Rudenski, S. F. Ziegler, D. R. Littman, TGF- β -induced Foxp3 inhibits T_H17 cell differentiation by antagonizing ROR γ t function. *Nature* **453**, 236–240 (2008).
- K. Ichijima, H. Yoshida, Y. Wakabayashi, T. Chinen, K. Saeki, M. Nakaya, G. Takaesu, S. Hori, A. Yoshimura, T. Kobayashi, Foxp3 inhibits ROR γ t-mediated IL-17A mRNA transcription through direct interaction with ROR γ t. *J. Biol. Chem.* **283**, 17003–17008 (2008).
- Z. Chen, A. Laurence, Y. Kanno, M. Pacher-Zavisin, B.-M. Zhu, C. Tato, A. Yoshimura, L. Hennighausen, J. J. O'Shea, Selective regulatory function of Socs3 in the formation of IL-17-secreting T cells. *Proc. Natl. Acad. Sci. U.S.A.* **103**, 8137–8142 (2006).
- D. M. Floss, S. Mrotzek, T. Klöcker, J. Schröder, J. Grötzinger, S. Rose-John, J. Scheller, Identification of canonical tyrosine-dependent and non-canonical tyrosine-independent STAT3 activation sites in the intracellular domain of the interleukin 23 receptor. *J. Biol. Chem.* **288**, 19386–19400 (2013).
- P. S. Biswas, S. Gupta, E. Chang, L. Song, R. A. Storzaker, J. K. Liao, G. Bhagat, A. B. Pernis, Phosphorylation of IRF4 by ROCK2 regulates IL-17 and IL-21 production and the development of autoimmunity in mice. *J. Clin. Invest.* **120**, 3280–3295 (2010).
- B. U. Schraml, K. Hildner, W. Ise, W.-L. Lee, W. A.-E. Smith, B. Solomon, G. Sahota, J. Sim, R. Mukasa, S. Cemerski, R. D. Hatton, G. D. Stormo, C. T. Weaver, J. H. Russell, T. L. Murphy, K. M. Murphy, The AP-1 transcription factor *Batf* controls T_H17 differentiation. *Nature* **460**, 405–409 (2009).
- L. Lebson, A. Gocke, J. Rosenzweig, J. Alder, C. Civin, P. A. Calabresi, K. A. Whartenby, Cutting edge: The transcription factor Kruppel-like factor 4 regulates the differentiation of Th17 cells independently of ROR γ t. *J. Immunol.* **185**, 7161–7164 (2010).
- M. Veldhoen, K. Hirota, A. M. Westendorf, J. Buer, L. Dumoutier, J.-C. Renauld, B. Stockinger, The aryl hydrocarbon receptor links T_H17-cell-mediated autoimmunity to environmental toxins. *Nature* **453**, 106–109 (2008).
- G. Cui, X. Qin, L. Wu, Y. Zhang, X. Sheng, Q. Yu, H. Sheng, B. Xi, J. Z. Zhang, Y. Q. Zang, Liver X receptor (LXR) mediates negative regulation of mouse and human Th17 differentiation. *J. Clin. Invest.* **121**, 658–670 (2011).
- A. Kimura, T. Naka, K. Nohara, Y. Fujii-Kuriyama, T. Kishimoto, Aryl hydrocarbon receptor regulates Stat1 activation and participates in the development of Th17 cells. *Proc. Natl. Acad. Sci. U.S.A.* **105**, 9721–9726 (2008).
- W. Niedbala, J. C. Alves-Filho, S. Y. Fukada, S. M. Vieira, A. Mitani, F. Sonogo, A. Mirchandani, D. C. Nascimento, F. Q. Cunha, F. Y. Liew, Regulation of type 17 helper T-cell function by nitric oxide during inflammation. *Proc. Natl. Acad. Sci. U.S.A.* **108**, 9220–9225 (2011).
- J. Geginat, M. Paroni, S. Maglie, J. S. Alfen, I. Kastirp, P. Gruarin, M. De Simone, M. Pagani, S. Abrignani, Plasticity of human CD4 T cell subsets. *Front. Immunol.* **5**, 630 (2014).
- K. Diener, X. S. Wang, C. Chen, C. F. Meyer, G. Keesler, M. Zukowski, T.-H. Tan, Z. Yao, Activation of the c-Jun N-terminal kinase pathway by a novel protein kinase related to human germinal center kinase. *Proc. Natl. Acad. Sci. U.S.A.* **94**, 9687–9692 (1997).
- H.-C. Chuang, X. Wang, T.-H. Tan, MAP4K family kinases in immunity and inflammation. *Adv. Immunol.* **129**, 277–314 (2016).
- H.-C. Chuang, J.-L. Lan, D.-Y. Chen, C.-Y. Yang, Y.-M. Chen, J.-P. Li, C.-Y. Huang, P.-E. Liu, X. Wang, T.-H. Tan, The kinase GLK controls autoimmunity and NF- κ B signaling by activating the kinase PKC- θ in T cells. *Nat. Immunol.* **12**, 1113–1118 (2011).
- D.-Y. Chen, H.-C. Chuang, J.-L. Lan, Y.-M. Chen, W.-T. Hung, K.-L. Lai, T.-H. Tan, Germinal center kinase-like kinase (GLK/MAP4K3) expression is increased in adult-onset Still's disease and may act as an activity marker. *BMC Med.* **10**, 84 (2012).
- Y.-M. Chen, H.-C. Chuang, W.-C. Lin, C.-Y. Tsai, C.-W. Wu, N.-R. Gong, W.-T. Hung, T.-H. Lan, J.-L. Lan, T.-H. Tan, D.-Y. Chen, Germinal center kinase-like kinase overexpression in T cells as a novel biomarker in rheumatoid arthritis. *Arthritis Rheum.* **65**, 2573–2582 (2013).
- R. Jain, Y. Chen, Y. Kanno, B. Joyce-Shaikh, G. Vahedi, K. Hirahara, W. M. Blumenschein, S. Sukumar, C. J. Haines, S. Sadekova, T. K. McClanahan, M. J. McGeachy, J. J. O'Shea, D. J. Cua, Interleukin-23-induced transcription factor blimp-1 promotes pathogenicity of T helper 17 cells. *Immunity* **44**, 131–142 (2016).
- F. Zhang, G. Meng, W. Strober, Interactions among the transcription factors Runx1, ROR γ t and Foxp3 regulate the differentiation of interleukin 17-producing T cells. *Nat. Immunol.* **9**, 1297–1306 (2008).
- T. Ikuta, Y. Kobayashi, K. Kawajiri, Phosphorylation of nuclear localization signal inhibits the ligand-dependent nuclear import of aryl hydrocarbon receptor. *Biochem. Biophys. Res. Commun.* **317**, 545–550 (2004).
- C. Wu, N. Yosef, T. Thalhammer, C. Zhu, S. Xiao, Y. Kishi, A. Regev, V. K. Kuchroo, Induction of pathogenic T_H17 cells by inducible salt-sensing kinase SGK1. *Nature* **496**, 513–517 (2013).
- X. K. Liu, J. L. Clements, S. L. Gaffen, Signaling through the murine T cell receptor induces IL-17 production in the absence of costimulation, IL-23 or dendritic cells. *Mol. Cells* **20**, 339–347 (2005).
- J. Gomez-Rodriguez, N. Sahu, R. Handon, T. S. Davidson, S. M. Anderson, M. R. Kirby, A. August, P. L. Schwartzberg, Differential expression of IL-17A and IL-17F is coupled to TCR signaling via Itk-mediated regulation of NFATc1. *Immunity* **31**, 587–597 (2009).
- N. Manel, D. Unutmaz, D. R. Littman, The differentiation of human T_H17 cells requires transforming growth factor- β and induction of the nuclear receptor ROR γ t. *Nat. Immunol.* **9**, 641–649 (2008).
- N. Yosef, A. K. Shalek, J. T. Gaubblomme, H. Jin, Y. Lee, A. Awasthi, C. Wu, K. Karwacz, S. Xiao, M. Jorgolli, D. Gennert, R. Satija, A. Shakya, D. Y. Lu, J. J. Trombetta, M. R. Pillai, P. J. Ratcliffe, M. L. Coleman, M. Bix, D. Tantin, H. Park, V. K. Kuchroo, A. Regev, Dynamic regulatory network controlling T_H17 cell differentiation. *Nature* **496**, 461–468 (2013).
- Q. Ruan, V. Kameswaran, Y. Zhang, S. Zheng, J. Sun, J. Wang, J. DeVirgiliis, H.-C. Liou, A. Beg, Y. H. Chen, The Th17 immune response is controlled by the Rel–ROR γ –ROR γ t transcriptional axis. *J. Exp. Med.* **208**, 2321–2333 (2011).
- J. Yang, P. Xu, L. Han, Z. Guo, X. Wang, Z. Chen, J. Nie, S. Yin, M. Piccioni, A. Tsun, L. Lv, S. Ge, B. Li, Cutting edge: Ubiquitin-specific protease 4 promotes Th17 cell function under inflammation by deubiquitinating and stabilizing ROR γ t. *J. Immunol.* **194**, 4094–4097 (2015).
- E. Zhu, X. Wang, B. Zheng, Q. Wang, J. Hao, S. Chen, Q. Zhao, L. Zhao, Z. Wu, Z. Yin, miR-20b suppresses Th17 differentiation and the pathogenesis of experimental autoimmune encephalomyelitis by targeting ROR γ t and STAT3. *J. Immunol.* **192**, 5599–5609 (2014).
- Q. Wu, J. Nie, Y. Gao, P. Xu, Q. Sun, J. Yang, L. Han, Z. Chen, X. Wang, L. Lv, A. Tsun, J. Shen, B. Li, Reciprocal regulation of ROR γ t acetylation and function by p300 and HDAC1. *Sci. Rep.* **5**, 16355 (2015).
- A. Yeste, I. D. Maccanfroni, M. Nadeau, E. J. Burns, A.-M. Tukpah, A. Santiago, C. Wu, B. Patel, D. Kumar, F. J. Quintana, IL-21 induces IL-22 production in CD4⁺ T cells. *Nat. Commun.* **5**, 3753 (2014).
- M. Lochner, L. Peduto, M. Cherrier, S. Sawa, F. Langa, R. Varona, D. Riethmacher, M. Si-Tahar, J. P. Di Santo, G. Eberl, In vivo equilibrium of proinflammatory IL-17⁺ and regulatory IL-10⁺ Foxp3⁺ ROR γ t⁺ T cells. *J. Exp. Med.* **205**, 1381–1393 (2008).
- Z. He, F. Wang, J. Ma, S. Sen, J. Zhang, Y. Gwack, Y. Zhou, Z. Sun, Ubiquitination of ROR γ t at lysine 446 limits Th17 differentiation by controlling coactivator recruitment. *J. Immunol.* **197**, 1148–1158 (2016).

42. Z. He, J. Ma, R. Wang, J. Zhang, Z. Huang, F. Wang, S. Sen, E. V. Rothenberg, Z. Sun, A two-amino-acid substitution in the transcription factor ROR γ t disrupts its function in Th17 differentiation but not in thymocyte development. *Nat. Immunol.* **18**, 1128–1138 (2017).
43. D. J. McGuire, A. L. Rowse, H. Li, B. J. Peng, C. M. Sestero, K. S. Cashman, P. De Sarno, C. Raman, CD5 enhances Th17-cell differentiation by regulating IFN- γ response and ROR γ t localization. *Eur. J. Immunol.* **44**, 1137–1142 (2014).
44. P. R. Taylor, S. Roy, S. M. Leal Jr., Y. Sun, S. J. Howell, B. A. Cobb, X. Li, E. Pearlman, Activation of neutrophils by autocrine IL-17A–IL-17RC interactions during fungal infection is regulated by IL-6, IL-23, ROR γ t and dectin-2. *Nat. Immunol.* **15**, 143–151 (2014).
45. F. J. Quintana, A. S. Basso, A. H. Iglesias, T. Korn, M. F. Farez, E. Bettelli, M. Caccamo, M. Oukka, H. L. Weiner, Control of T_{reg} and Th17 cell differentiation by the aryl hydrocarbon receptor. *Nature* **453**, 65–71 (2008).
46. P. P. Ho, L. Steinman, The aryl hydrocarbon receptor: A regulator of Th17 and Treg cell development in disease. *Cell Res.* **18**, 605–608 (2008).
47. M. Veldhoen, K. Hirota, J. Christensen, A. O'Garra, B. Stockinger, Natural agonists for aryl hydrocarbon receptor in culture medium are essential for optimal differentiation of Th17 T cells. *J. Exp. Med.* **206**, 43–49 (2009).
48. N. Hermann-Kleiter, G. Baier, NFAT pulls the strings during CD4⁺ T helper cell effector functions. *Blood* **115**, 2989–2997 (2010).
49. A. Schmidt, N. Oberle, P. H. Kramer, Molecular mechanisms of Treg-mediated T cell suppression. *Front. Immunol.* **3**, 51 (2012).
50. S. Krishna, D. Xie, B. Gorenz, J. Shin, J. Gao, X.-P. Zhong, Chronic activation of the kinase IKK β impairs T cell function and survival. *J. Immunol.* **189**, 1209–1219 (2012).
51. I. Backert, S. B. Koralov, S. Wirtz, V. Kitowski, U. Billmeier, E. Martini, K. Hofmann, K. Hildner, N. Wittkopf, K. Brecht, M. Waldner, K. Rajewsky, M. F. Neurath, C. Becker, C. Neufert, STAT3 activation in Th17 and Th22 cells controls IL-22-mediated epithelial host defense during infectious colitis. *J. Immunol.* **193**, 3779–3791 (2014).
52. L. Wei, A. Laurence, K. M. Elias, J. J. O'Shea, IL-21 is produced by Th17 cells and drives IL-17 production in a STAT3-dependent manner. *J. Biol. Chem.* **282**, 34605–34610 (2007).
53. R. Nurieva, X. O. Yang, G. Martinez, Y. Zhang, A. D. Panopoulos, L. Ma, K. Schluns, Q. Tian, S. S. Watowich, A. M. Jetten, C. Dong, Essential autocrine regulation by IL-21 in the generation of inflammatory T cells. *Nature* **448**, 480–483 (2007).
54. C. P. Hsu, H. C. Chuang, M. C. Lee, H. H. Tsou, L. W. Lee, J. P. Li, T. H. Tan, GLK/MAP4K3 overexpression associates with recurrence risk for non-small cell lung cancer. *Oncotarget* **7**, 41748–41757 (2016).
55. C. H. Ho, H. C. Chuang, I. C. Wu, H. W. Tsai, Y. J. Lin, H. Y. Sun, K. C. Young, Y. C. Chiu, P. N. Cheng, W. C. Liu, T. H. Tan, T. T. Chang, Prediction of early hepatocellular carcinoma recurrence using germinal center kinase-like kinase. *Oncotarget* **7**, 49765–49776 (2016).
56. R. M. Thomas, H. Sai, A. D. Wells, Conserved intergenic elements and DNA methylation cooperate to regulate transcription at the il17 locus. *J. Biol. Chem.* **287**, 25049–25059 (2012).
57. H.-C. Chuang, W. H.-H. Sheu, Y.-T. Lin, C.-Y. Tsai, C.-Y. Yang, Y.-J. Cheng, P.-Y. Huang, J.-P. Li, L.-L. Chiu, X. Wang, M. Xie, M. D. Schneider, T.-H. Tan, HGK/MAP4K4 deficiency induces TRAF2 stabilization and Th17 differentiation leading to insulin resistance. *Nat. Commun.* **5**, 4602 (2014).
58. E. Serfling, F. Berberich-Siebelt, S. Chuvpilo, E. Jankevics, S. Klein-Hessling, T. Twardzik, A. Avots, The role of NF-AT transcription factors in T cell activation and differentiation. *Biochim. Biophys. Acta* **1498**, 1–18 (2000).
59. S. J. Szabo, S. T. Kim, G. L. Costa, X. Zhang, C. G. Fathman, L. H. Glimcher, A novel transcription factor, T-bet, directs Th1 lineage commitment. *Cell* **100**, 655–669 (2000).

Acknowledgments: We thank the Transgenic Mouse Core (NHRI, Taiwan) for generation of Tg and KO mice. We thank the core facilities of NHRI (Taiwan) for tissue sectioning/H&E staining and confocal microscopy. We thank the Laboratory Animal Center (AAALAC-accredited) of NHRI for mouse housing. We thank the Institute of Biological Chemistry of Academia Sinica for MS. **Funding:** This work was supported by grants from NHRI, Taiwan (IM-105-PP-01 and IM-105-SP-01 to T.-H.T.) and the Ministry of Science and Technology, Taiwan (MOST-106-2321-B-400-013 to T.-H.T.). T.-H.T. is a Taiwan Bio-Development Foundation Chair in Biotechnology. **Author contributions:** H.-C.C. designed and performed experiments, analyzed and interpreted data, and wrote the manuscript. C.-Y.T. and C.-H.H. performed experiments and assisted in data interpretation. T.-H.T. conceived the study, supervised experiments, and wrote the manuscript. **Competing interests:** A provisional patent related to this work has been filed by NHRI with U.S. Patent Office, application no. 62719416. H.-C.C. and T.-H.T. are inventors of this application. The authors declare that they have no other competing interests. **Data and materials availability:** Correspondence and requests for materials should be addressed to T.-H.T. (ttan@nhri.org.tw). All data needed to evaluate the conclusions in the paper are present in the paper and/or the Supplementary Materials. Additional data related to this paper may be requested from the authors.

Submitted 9 March 2018

Accepted 24 July 2018

Published 12 September 2018

10.1126/sciadv.aat5401

Citation: H.-C. Chuang, C.-Y. Tsai, C.-H. Hsueh, T.-H. Tan, GLK-IKK β signaling induces dimerization and translocation of the AhR-ROR γ t complex in IL-17A induction and autoimmune disease. *Sci. Adv.* **4**, eaat5401 (2018).